

ELECTRONIC SUPPLEMENTARY INFORMATION

Enhanced electronic communication through a conjugated bridge in a porphyrin-fullerene donor-acceptor couple

Rubén Caballero,^a Joaquín Calbo,^b Juan Aragón,^b Pilar de la Cruz,^a Enrique Ortí,^{b,*} Nikolai Tkachenko,^{c,*} Fernando Langa^{a,*}

^a Instituto de Nanociencia, Nanotecnología y Materiales Moleculares (INAMOL), Universidad de Castilla-La Mancha, Campus de la Fábrica de Armas, 45071 Toledo, Spain; fernando.langa@uclm.esb

^b Instituto de Ciencia Molecular, Universidad de Valencia, 46950 Paterna, Spain; enrique.orti@uv.es

^c Faculty of Engineering and Natural Science, Tampere University, P.O. Box 541, Tampere 33101, Finland; nikolai.tkachenko@tuni.fi

Table of contents

1. Materials and methods.....	3
2. Synthesis.....	4
3. Computational methods.....	22
4. Molecular geometry and orbitals.....	23
5. Electrochemical properties and calculated Mulliken charges.....	25
6. Absorption and emission properties.....	28
7. Transient absorption spectra.....	34
8. References.....	37

1. Materials and methods.

C₆₀ buckminsterfullerene (+99.95%) was purchased from BuckyUSA (Bellaire, TX). Toluene, benzonitrile (PhCN) and 1,2-dichlorobenzene (o-DCB) were purchased from Aldrich Chemicals (Milwaukee, WI). Anhydrous solvents, where indicated, were dried using standard techniques. All other chemicals were used as received. Chromatographic purifications were performed using silica gel 60 VWR (particle size 0.040–0.063 mm) or basic activated alumina (Scharlab). Analytical thin-layer chromatography was performed using Merck TLC silica gel 60 F254. ¹H NMR spectra were recorded as CDCl₃ solutions on a Brüker-Topspin AV 400 instrument. Chemical shifts are given as δ values. Residual solvent peaks were used as the internal standard (CHCl₃; δ = 7.27 ppm). ¹³C NMR chemical shifts are reported relative to the solvent peak (CDCl₃, δ = 77.00 ppm). MALDI-TOF MS spectra were recorded on a VOYAGER DETM STR spectrometer from ABSciex using Dithranol as matrix. ESI-QTOF MS spectra were recorded in a 3200 QTRAP Spectrometer LC-MS/MS System from ABSciex. FT-IR spectra were recorded in an AVATAR 370 FT-IR Thermo Nicolet spectrometer. Steady-state UV-Vis measurements were carried out on a Shimadzu UV 3600 spectrophotometer. For extinction coefficient determination, solutions of different concentration were prepared in dichloromethane (DCM), HPLC grade, with absorbance between 0.1 and 1 using a 1 cm UV cuvette. Spectrochemical oxidation was carried out placing 3 mL of a 10⁻⁶ M solution of the sample and adding increasing amounts of a concentrated solution of FeCl₃ in dichloromethane. The volume of each addition was 3 μ L. The emission measurements were carried out on a Cary Eclipse fluorescence spectrophotometer. Cyclic and Oyster-Young square-wave voltammetry measurements were performed in 0.1 M solutions of tetrabutylammonium perchlorate in 1,2-dichlorobenzene:acetonitrile 4:1 as solvent. The concentration of the sample was 10⁻³ M. Solutions were deoxygenated by bubbling argon through prior to each measurement, which was run under argon atmosphere. Experiments were carried out in a one-compartment cell equipped with a glassy carbon electrode, a platinum-wire counter electrode and an Ag/0.01 M AgNO₃ as pseudo-reference electrode. All potentials were checked against the ferrocene/ferrocenium couple (Fc/Fc⁺) after each experiment.

2. Synthesis

Synthesis of 4. Under argon atmosphere, at 0 °C, **2** (166 mg, 0.16 mmol) was added over a suspension of NaH (16 mg, 0.66 mmol) in dry dimethylformamide (35 mL). After 15 minutes, a solution of **3** (120 mg, 0.33 mmol) in dry dimethylformamide (40 mL) was added and the mixture was stirred for 18 hours at room temperature. Then a mixture of ice and concentrated HCl was added and the solid formed was filtrated and washed with water. After drying, the crude was purified by column chromatography (silica gel hexane/dichloromethane 3:7) to obtain aldehyde **4** as a red solid (82 mg, 42% yield). ¹H NMR (400 MHz, CDCl₃) δ/ppm: 9.83 (s, 1H), 8.92 (d, 2H, *J* = 4.8 Hz), 8.77 (d, 2H, *J* = 4.8 Hz), 8.72 (s, 4H), 8.20 (d, 2H, *J* = 8.0 Hz), 7.84 (d, 2H, *J* = 8.0 Hz), 7.49 (d, 1H, *J* = 16.2 Hz), 7.29 (bs, 6H), 7.26 (d, 1H, *J* = 16.0 Hz), 7.19 (d, 1H, *J* = 16.2 Hz), 6.93 (d, 1H, *J* = 16.0 Hz), 4.40 (bs, 8H), 2.64 (s, 9H), 1.87 (s, 6H), 1.86 (s, 12 H). ¹³C NMR (100 MHz, CDCl₃) δ/ppm: 179.1, 149.9, 149.8, 149.7, 142.3, 141.0, 139.8, 139.3, 139.1, 138.9, 138.2, 137.4, 136.2, 134.9, 132.0, 131.1, 131.0, 130.6, 129.0, 127.6, 127.2, 124.4, 121.1, 119.7, 118.8, 118.6, 118.1, 117.9, 115.2, 115.0, 65.4, 65.1, 64.9, 64.6, 21.8, 21.7, 21.5, UV-Vis (dichloromethane), λ_{max}/nm (log ε): 422 (5.30), 478 (4.61), 550.5 (4.27). FT-IR (KBr) ν/cm⁻¹: 2980, 2914, 1645, 1440, 1079, 993. MS (MALDI-TOF) m/z: calculated for C₇₀H₅₈N₄O₅S₂Zn: 1162.31; found: 1162.47 (M⁺).

Synthesis of 1. Under argon atmosphere, a solution of **4** (70 mg, 0.06 mmol), C₆₀ (42 mg, 0.04 mmol) and *N*-methylglycine (16 mg, 0.16mmol) in anhydrous chlorobenzene (36 mL) was heated to reflux for 5 hours. After cooling to room temperature, the solvent was evaporated and the crude was purified by column chromatography (silica gel, toluene:hexane 1:1) and gel permeation chromatography (Biobeads SX1, toluene). The solid obtained was washed several times with methanol and n-pentane to afford pure **1** as a red solid (50 mg, 44% yield). ¹H NMR (400 MHz, CDCl₃) δ/ppm: 8.92 (d, 2H, *J* = 4.6 Hz), 8.76 (d, 2H, *J* = 4.6 Hz), 8.72 (s, 4H), 8.18 (d, 2H, *J* = 8.0 Hz), 7.82 (d, 2H, *J* = 8.0 Hz), 7.47 (d, 1H, *J* = 16.0 Hz), 7.28 (s, 6H), 7.13 (d, 1H, *J* = 16.0 Hz), 7.02 (d, 1H, *J* = 16.0 Hz), 6.94 (d, 1H, *J* = 16.0 Hz), 5.43 (bs, 1H), 4.98 (d, 1H, *J* = 9.2 Hz), 4.36–4.12 (m, 8H), 4.23 (d, 1H, *J* = 9.2 Hz), 2.96 (s, 3H), 2.63 (s, 9H), 1.87 (s, 6H), 1.86 (s, 12H). ¹³C NMR (100 MHz, CDCl₃) δ/ppm: 156.0, 153.7, 153.6, 153.1, 149.8, 149.7, 147.0, 146.6, 146.3, 146.2, 146.0, 145.9, 145.8, 145.6, 145.3, 145.2, 145.1, 145.1, 145.0, 144.9, 144.4, 144.1,

evaporated and dichloromethane and water added. Phases were separated and the organic phase washed with water. The organic phases were dried and evaporated and the crude mixture purified by column chromatography (alumina, toluene 1:1) to obtain **S9** as a yellow solid. (0.44 g, 70% yield). ¹H NMR (400 MHz, CDCl₃) δ/ppm: 7.47 (d, 2H, *J* = 7.4 Hz), 7.34 (t, 2H, *J* = 7.4 Hz), 7.23 (t, 1H, *J* = 7.4 Hz), 7.17 (d, 1H, *J* = 16.2 Hz), 6.88 (d, 1H, *J* = 16.2 Hz), 6.24 (s, 1H), 4.29 (m, 2H), 4.23 (m, 2H). FT-IR (neat-ATR) ν/cm⁻¹: 1477, 1426, 1362, 1267, 1163, 1074, 960, 903, 751, 754, 583, 539. MS (ESI-QTOF) *m/z*: calculated for C₁₄H₁₂O₂S: 244.05; Found: 245.1 (M-H⁺).

Synthesis of S10. Under argon atmosphere, at 0 °C, phosphorus(V) oxychloride (0.4 mL, 3.6 mmol) was added over a solution of dimethylformamide (0.9 mL, 10.7 mmol) in dry dichloromethane (30 mL) and the mixture was stirred for 15 min at this temperature. Over this reaction mixture, at the same temperature, a solution of **S9** (0.43 g, 1.8 mmol) in dry dichloromethane (60 mL) was added dropwise, then the reaction mixture was heated to reflux for 3 hours. After this time, the reaction mixture was poured into ice and neutralized with a saturated solution of NaHCO₃. Phases were separated, and the organic phase was washed with water and then dried and evaporated. The crude product was purified by column chromatography (alumina, chloroform) to obtain **S10** as a yellow solid (0.38 g, 80%). ¹H NMR (400 MHz, CDCl₃) δ/ppm: 9.89 (s, 1H), 7.49 (d, 2H, *J* = 7.4 Hz), 7.36 (t, 2H, *J* = 7.4 Hz), 7.29 (t, 1H, *J* = 7.2 Hz), 7.16 (d, 1H, *J* = 16.2 Hz), 7.10(d, 1H, *J* = 16.2 Hz), 4.37 (m, 2H), 4.36 (m, 2H). ¹³C NMR (100 MHz, CDCl₃) δ/ppm: 179.4, 148.7, 138.7, 136.2, 131.5, 128.7, 128.5, 128.0, 126.7, 117.2, 115.4, 65.3, 64.5.

Synthesis of Ph-2EDOTV (5). Under argon atmosphere, at 0 °C, NaH (60% dispersion in mineral oil, 0.044 g, 1.1 mmol) was added dropwise over a stirred solution of **S11**³ (0.16 g, 0.55 mmol) in dry dimethylformamide (5 mL) and the mixture was stirred at the same temperature for 15 minutes. After, a solution of **S10** (0.1 g, 0.37 mmol) in dry dimethylformamide (5 mL) was added dropwise and the reaction was allowed to warm and stirred 16 hours at room temperature. After this time a drop of water was added, and the solvent was evaporated under reduced pressure. The crude product was purified by column chromatography (alumina, toluene) and the obtained solid washed with cyclohexane to obtain **5** as a yellow solid (0.23 g, 82%). ¹H NMR (400 MHz, CDCl₃) δ/ppm: 7.45 (d, 2H, *J* = 7.6 Hz), 7.33 (t, 2H, *J* = 7.6 Hz), 7.22 (t, 1H, *J* = 7.3 Hz), 7.17 (d, 1H, *J* = 16.1 Hz), 6.92 (d, 1H, *J* = 16.0 Hz), 6.86 (d, 1H, *J* = 16.0 Hz), 6.71 (d, 1H, *J* = 16.1 Hz), 6.21 (s, 1H), 4.30 (m, 4H), 4.28 (m, 2H), 4.22 (m, 2H). ¹³C NMR (100 MHz, CDCl₃) δ/ppm: 141.9,

139.5, 139.0, 138.9, 137.4, 128.6, 127.1, 126.1, 125.9, 117.8, 117.4, 116.3, 115.9, 115.6, 115.1, 97.5, 64.9, 64.8, 64.7, 64.7. FT-IR (neat-ATR) ν/cm^{-1} : 1505, 1445, 1356, 1264, 1173, 1174, 929, 755, 685. UV-Vis (dichloromethane) $\lambda_{\text{max}}/\text{nm}$ (log ϵ): 312 (3.86), 424 (4.31). MS (ESI-QTOF) m/z : calculated for $\text{C}_{22}\text{H}_{18}\text{O}_4\text{S}_2$: 410.06; Found: 410.3 (M^+).

Synthesis of S12. Under argon atmosphere, at 0 °C, phosphorus(V) oxychloride (0.1 mL, 0.8 mmol) was added over a solution of dimethylformamide (0.2 mL, 2.5 mmol) in dry dichloromethane (7 mL) and the mixture was stirred for 15 min at this temperature. Over this reaction mixture, at the same temperature, a solution of **5** (0.17 g, 0.4 mmol) in dry dichloromethane (10 mL) was added dropwise; then, the reaction mixture was heated to reflux for 3 hours. After this time, the reaction mixture was poured into ice and neutralized with a saturated solution of NaHCO_3 . Phases were separated, and the organic phase was washed with water and then dried and evaporated. The crude product was purified by column chromatography (alumina, chloroform) and the solid obtained washed with cyclohexane to obtain **S12** as a red solid (0.10 g, 55%). ^1H NMR (400 MHz, CDCl_3) δ/ppm : 9.88 (s, 1H), 7.47 (d, 2H, $J = 7.6$ Hz), 7.34 (t, 2H, $J = 7.5$ Hz), 7.25 (t, 1H, $J = 7.6$ Hz), 7.20 (d, 1H, $J = 16.0$ Hz), 7.16 (d, 1H, $J = 16.0$ Hz), 6.86 (d, 2H, $J = 16.0$ Hz), 4.36 (m, 8H). ^{13}C NMR (100 MHz, CDCl_3) δ/ppm : 192.5, 179.15, 140.9, 139.6, 138.2, 137.1, 128.7, 127.5, 127.2, 126.2, 121.10, 117.7, 117.6, 115.0, 114.9, 114.8, 65.4, 65.0, 64.8, 64.6. FT-IR (neat-ATR) ν/cm^{-1} : 1635, 1502, 1435, 1372, 1255, 1084, 957, 701, 669. MS (ESI-QTOF) m/z : calculated for $\text{C}_{23}\text{H}_{18}\text{O}_5\text{S}_2$: 438.06; Found: 439.9 (M-H^+).

Synthesis of Ph-2EDOTV-C₆₀ (6). Under argon atmosphere, a solution of (39 mg, 0.09 mmol), C_{60} (192 mg, 0.27 mmol) and N-methylglycine (50 mg, 0.53 mmol) in anhydrous chlorobenzene (15 mL) was heated to reflux for 4 hours. After cooling to room temperature, the solvent was evaporated and the crude was purified by column chromatography (silica gel, toluene). The solid obtained was washed several times with methanol and n-pentane to afford pure **6** as a brown solid (54 mg, 55% yield). ^1H NMR (400 MHz, $\text{CDCl}_3/\text{CS}_2$ 1:1) δ/ppm : 7.40 (d, 2H, $J = 7.4$ Hz), 7.30 (t, 2H, $J = 7.7$ Hz), 7.19 (t, 1H, $J = 7.4$ Hz), 7.11 (d, 1H, $J = 16.1$ Hz), 6.88 (d, 1H, $J = 15.9$ Hz), 6.81 (d, 1H, $J = 15.9$ Hz), 6.75 (d, 1H, $J = 16.1$ Hz), 5.42 (bs, 1H), 4.96 (d, 1H, $J = 9.5$ Hz), 4.29 (m, 8H), 4.23 (d, 1H, $J = 9.5$ Hz), 2.94 (s, 3H). ^{13}C NMR (100 MHz, $\text{CDCl}_3/\text{CS}_2$ 1:1) δ/ppm : 155.9, 153.6, 153.5, 153.0, 147.2, 147.1, 146.5, 146.3, 146.2, 146.1, 146.0, 145.9, 145.8, 145.7, 145.6, 145.5, 145.4, 145.3, 145.2, 145.1, 145.0, 144.9, 144.5, 144.4, 144.2, 144.1, 143, 142.8, 142.5,

142.4, 142.1, 142.0, 140.0, 139.9, 139.7, 139.6, 139.4, 139.0, 138.0, 137.2, 137.0, 136.5, 135.6, 135.3, 130.4, 128.5, 127.0, 126.0, 125.9, 118.3, 117.6, 116.4, 116.0, 115.9, 115.5, 69.6, 68.7, 64.8, 64.7, 40.3, 29.8. FT-IR (KBr) ν/cm^{-1} : 2923, 2857, 2771, 1584, 1432, 1356, 1081, 951, 736, 691, 520. UV-Vis (dichloromethane), λ_{max} (log ϵ): 321 (4.62), 435 (4.52) nm. MS (ESI-QTOF) m/z : calculated for $\text{C}_{85}\text{H}_{23}\text{NO}_4\text{S}_2$: 1185.1; Found: 1186.2 (M-H⁺). UV-Vis (dichloromethane), λ_{max} (log ϵ): 321 (4.62), 435 (4.52) nm.

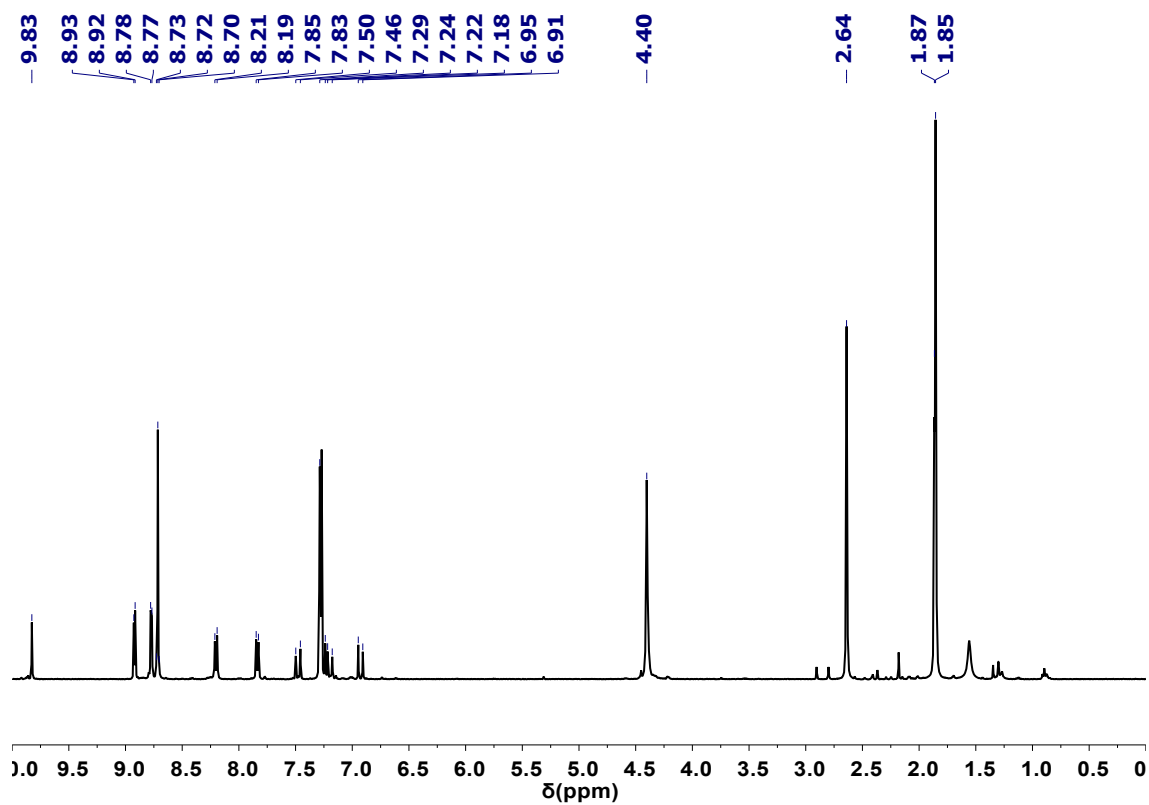


Figure S1. ^1H NMR (400 MHz, CDCl_3), spectrum of compound 4.

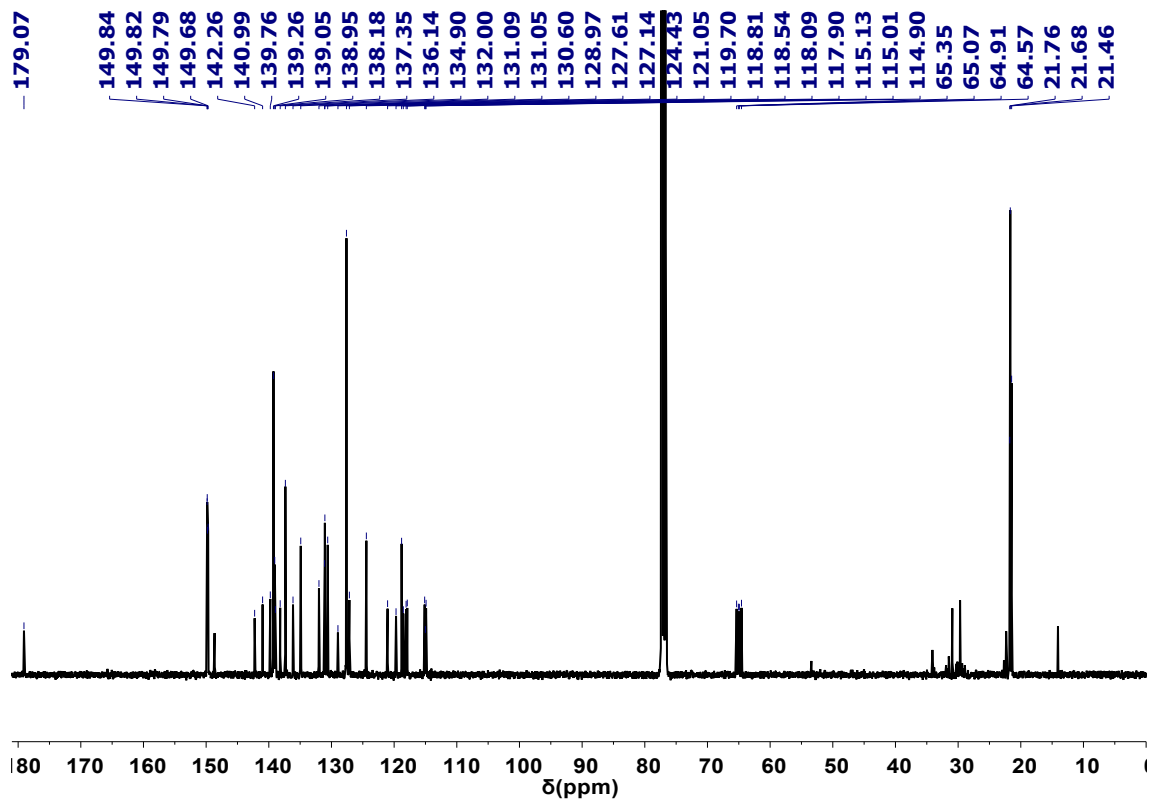


Figure S2. ^{13}C NMR (100 MHz, CDCl_3) spectrum of compound 4.

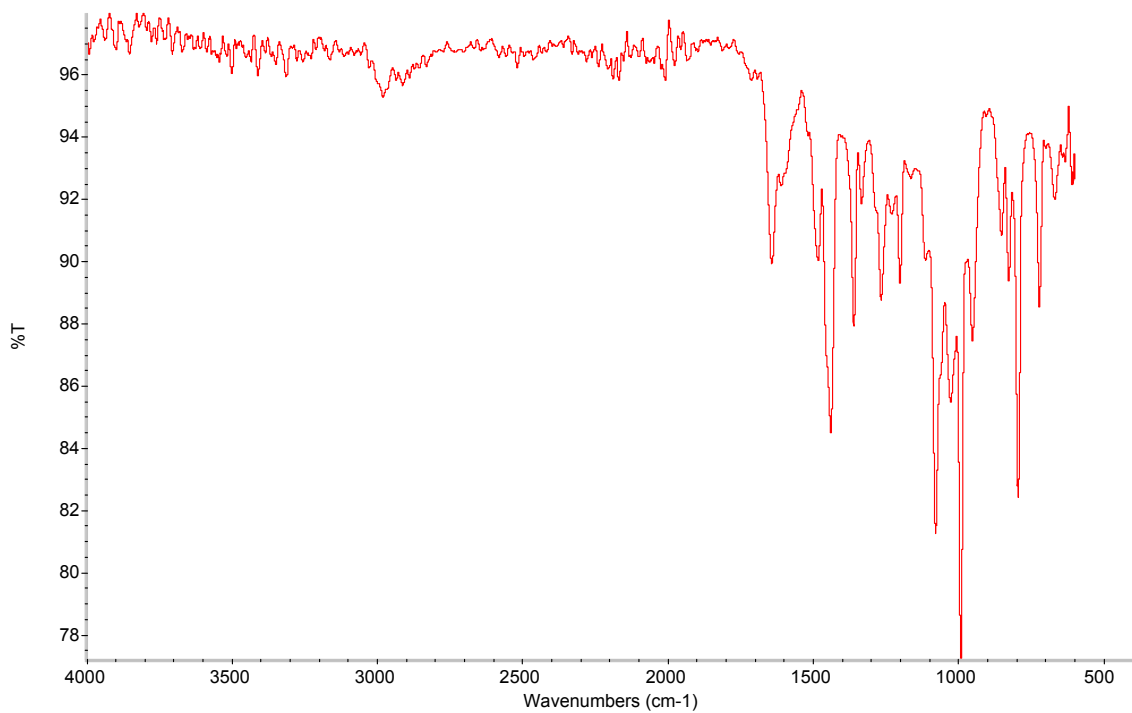


Figure S3. FT-IR (neat-ATR) spectrum of compound 4.

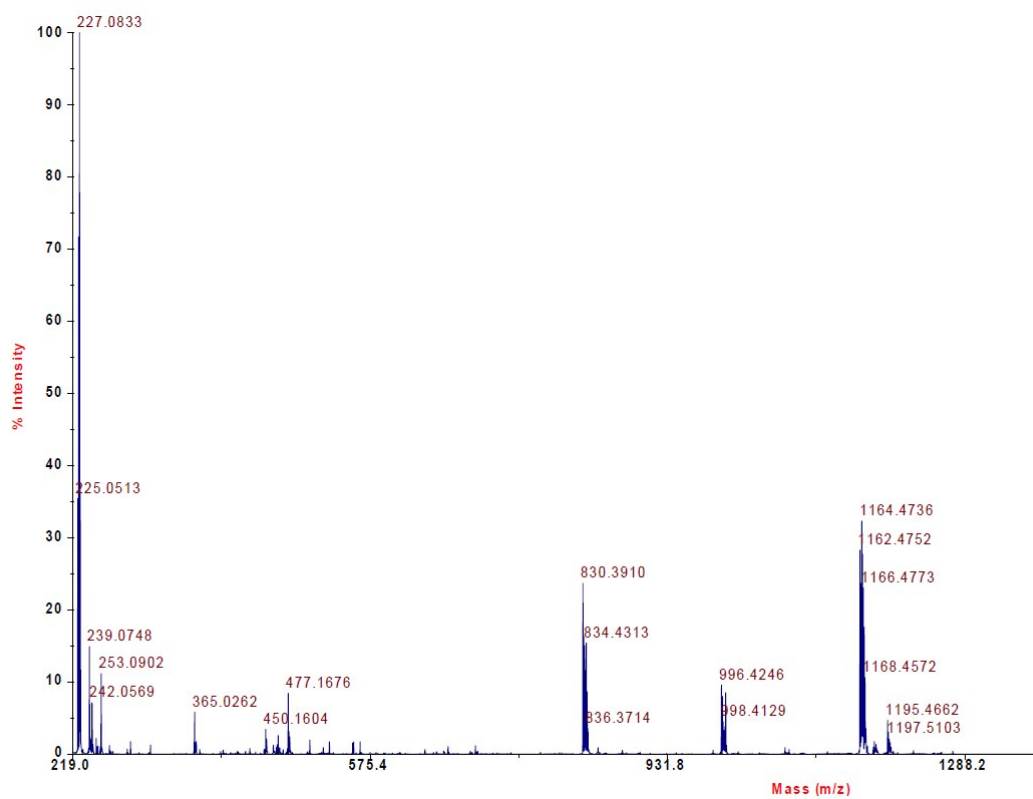


Figure S4. MS (MALDI-TOF) spectrum of compound 4.

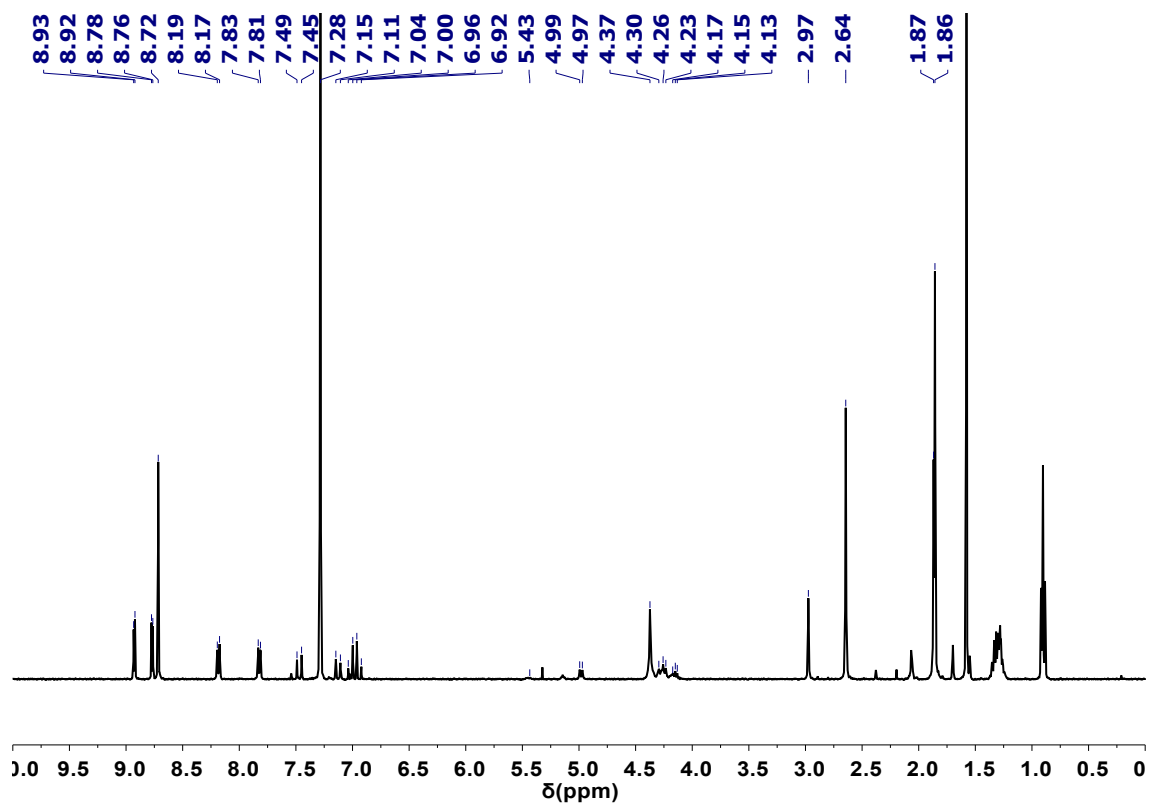


Figure S5. ^1H NMR (400 MHz, CDCl_3) spectrum of compound ZnP-2EDOTV- C_{60} (**1**).

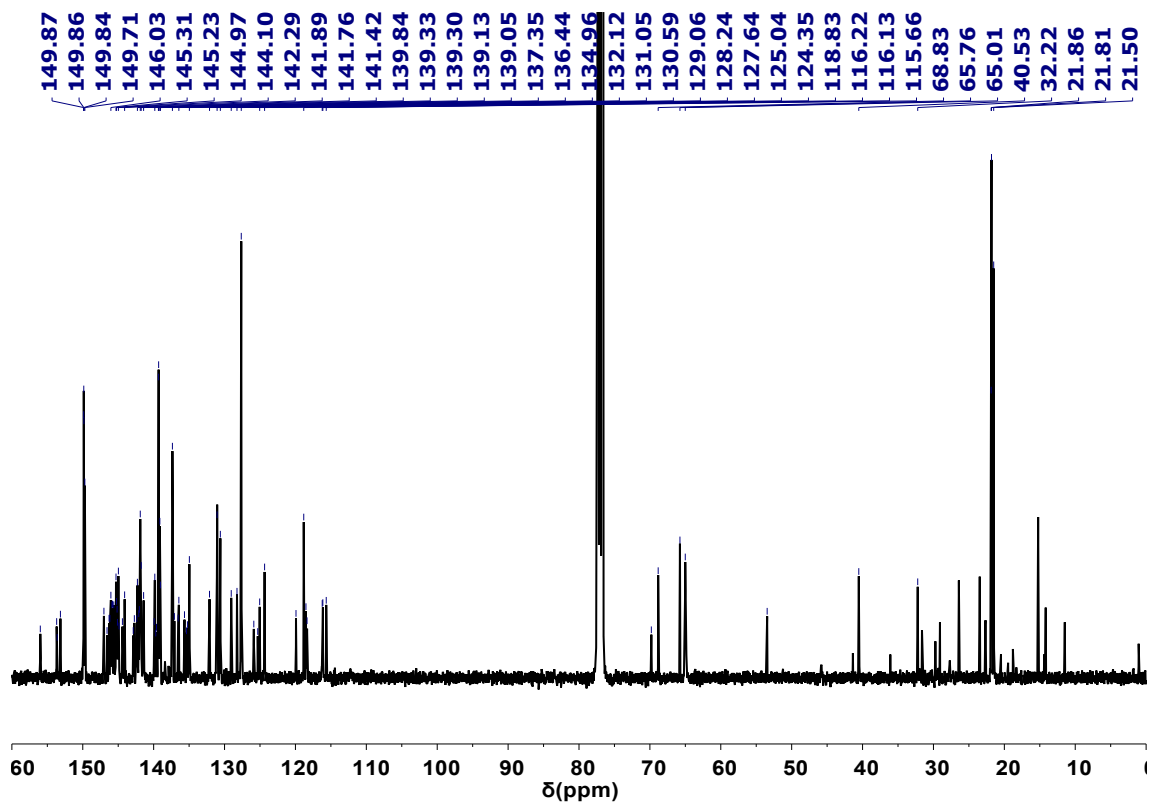


Figure S6. ^{13}C NMR (100 MHz, CDCl_3) spectrum of compound ZnP-2EDOTV- C_{60} (**1**).

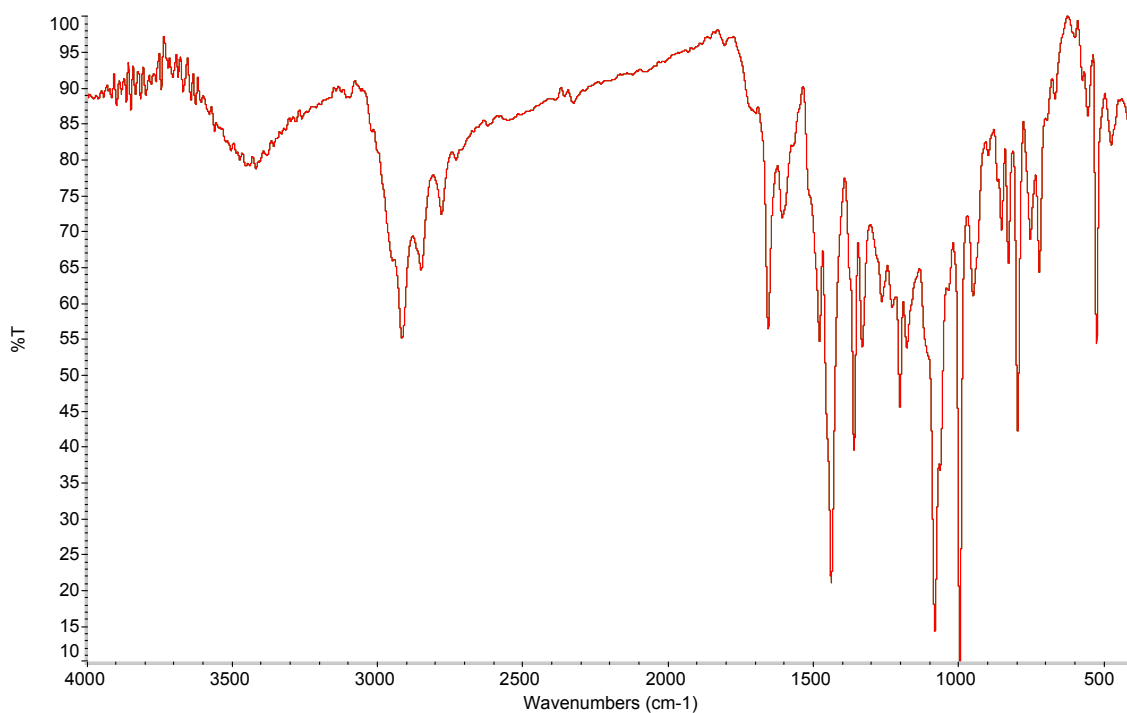


Figure S7. FT-IR (KBr) spectrum of compound ZnP-2EDOTV-C₆₀ (**1**).

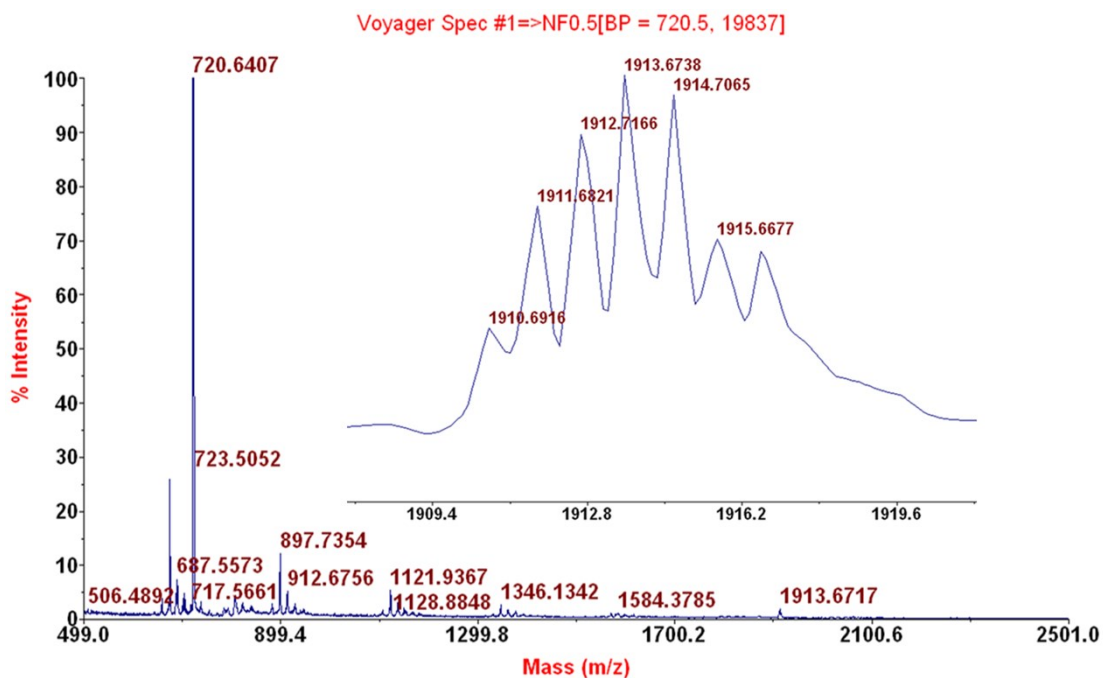


Figure S8. MS (MALDI-TOF) spectrum of compound ZnP-2EDOTV-C₆₀ (**1**).

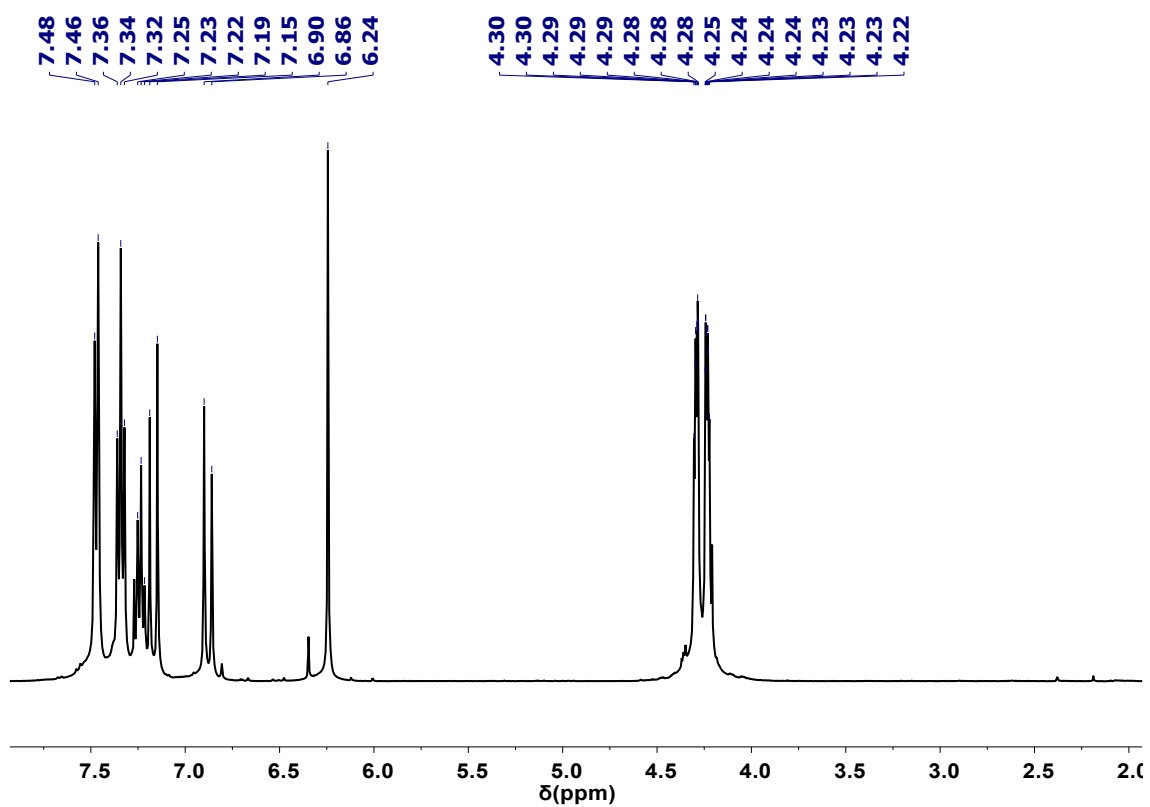


Figure S9. ^1H NMR (400MHz, CDCl_3) spectrum of compound **S9**.

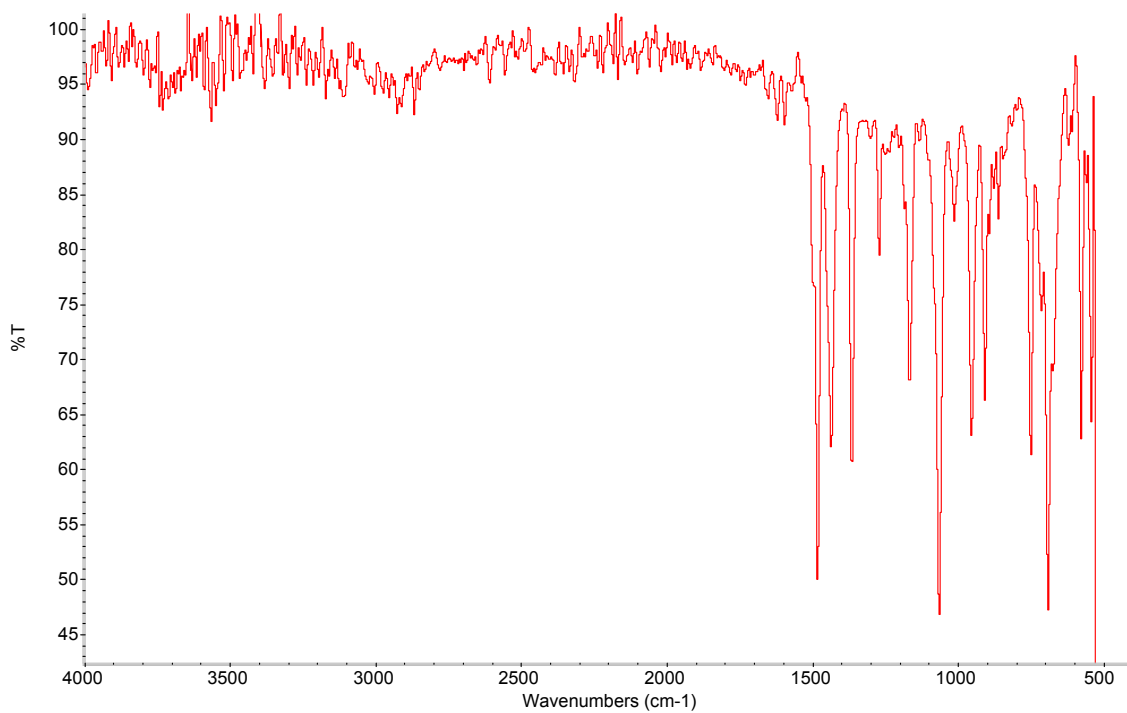


Figure S10. FT-IR (neat-ATR) spectrum of compound **S9**.

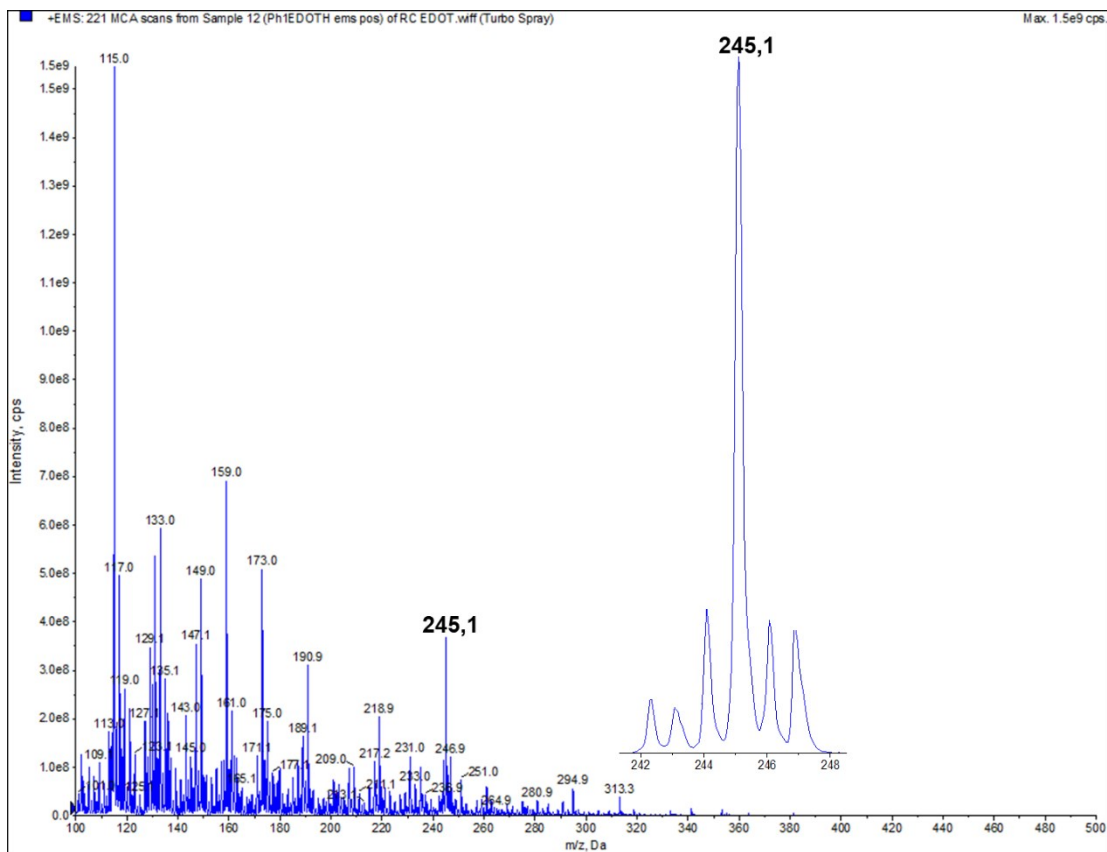


Figure S11. MS (ESI-QTOF) spectrum of compound S9.

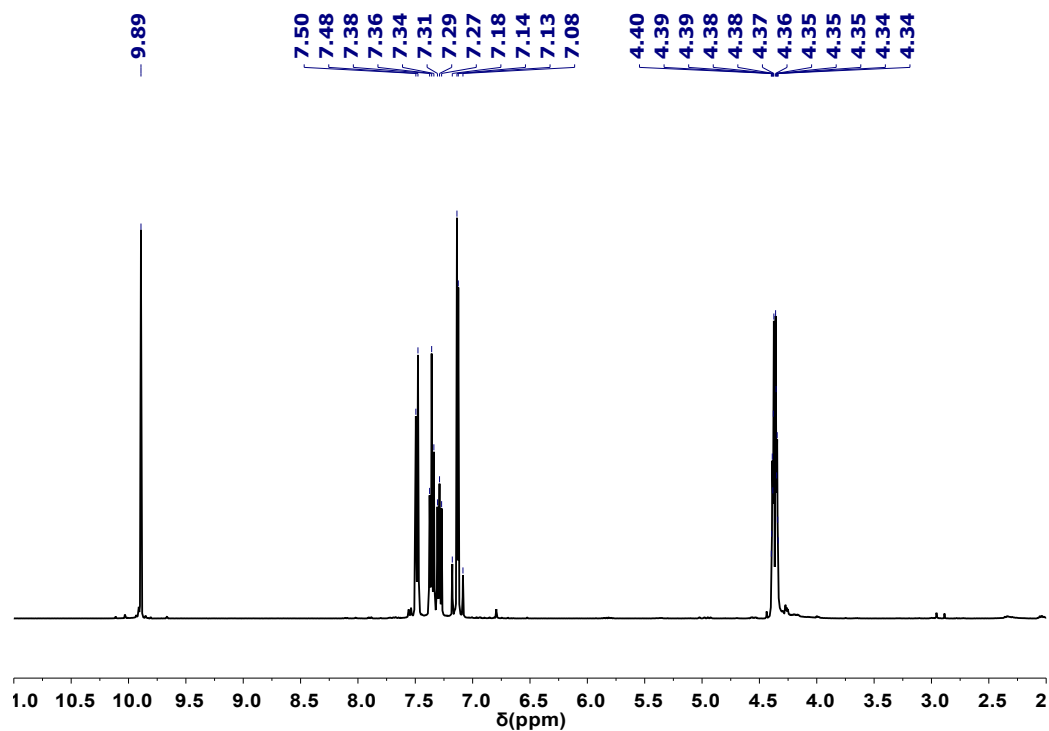


Figure S12. ¹H NMR (400 MHz, CDCl₃) spectrum of compound S10.

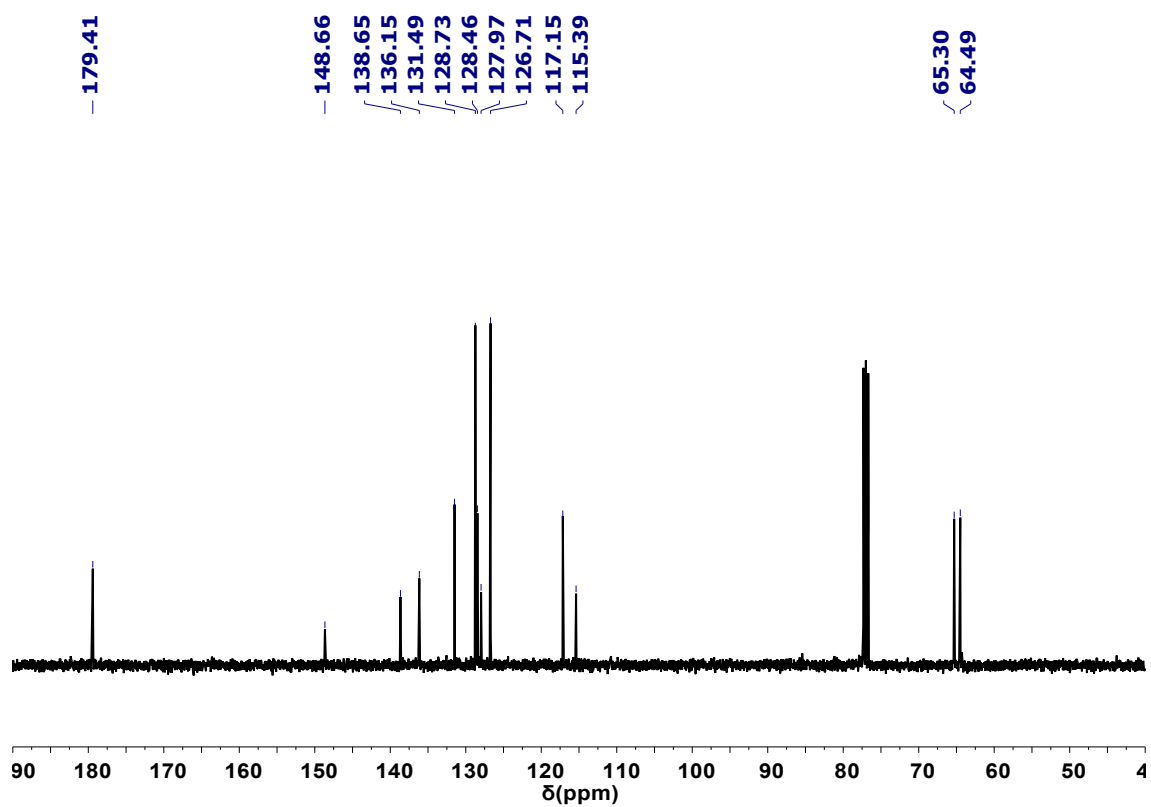


Figure S13. ^{13}C NMR (100 MHz, CDCl_3) spectrum of compound S10.

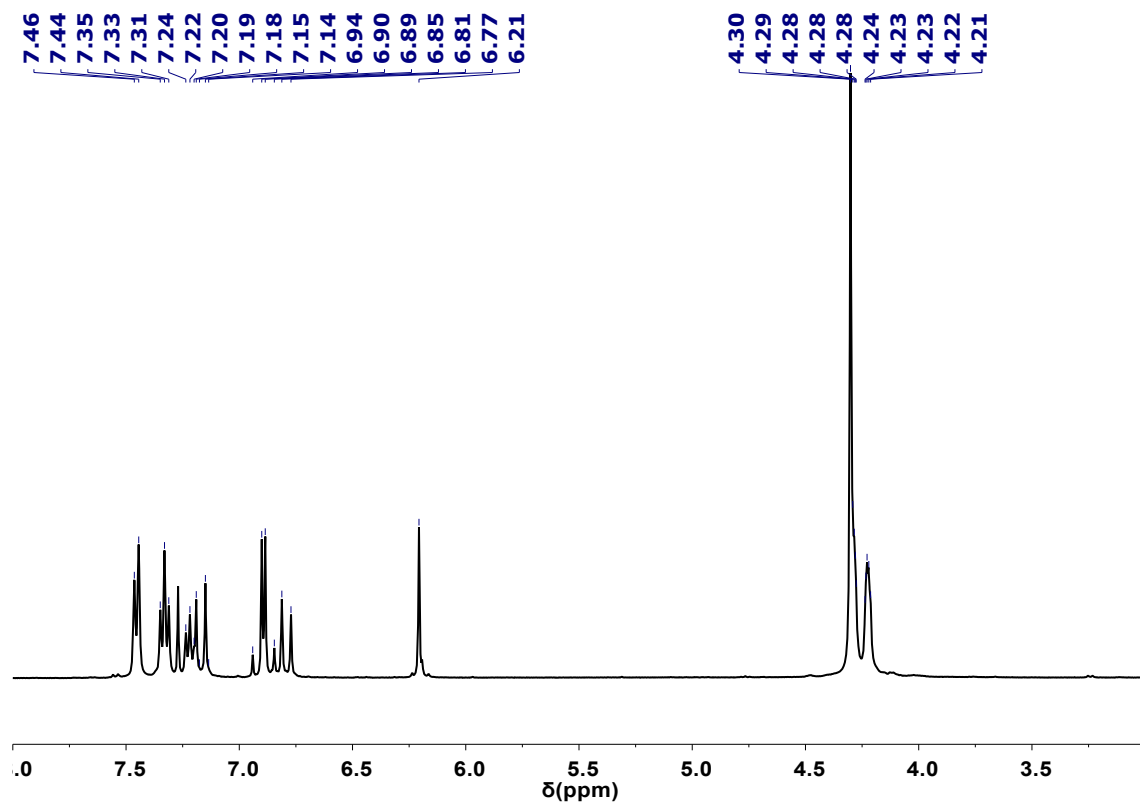


Figure S14. ^1H NMR (400 MHz, CDCl_3) spectrum of compound Ph-2EDOTV (5).

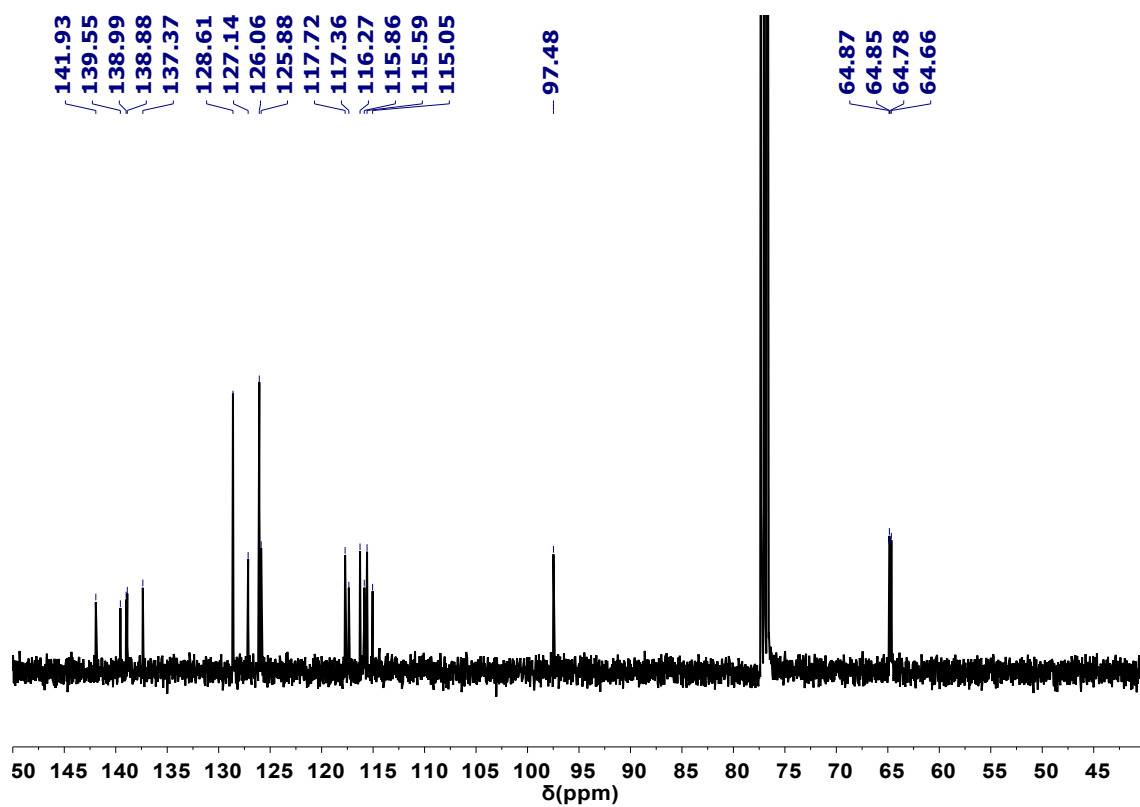


Figure S15. ^{13}C NMR (100 MHz, CDCl_3) spectrum of compound Ph-2EDOTV (**5**).

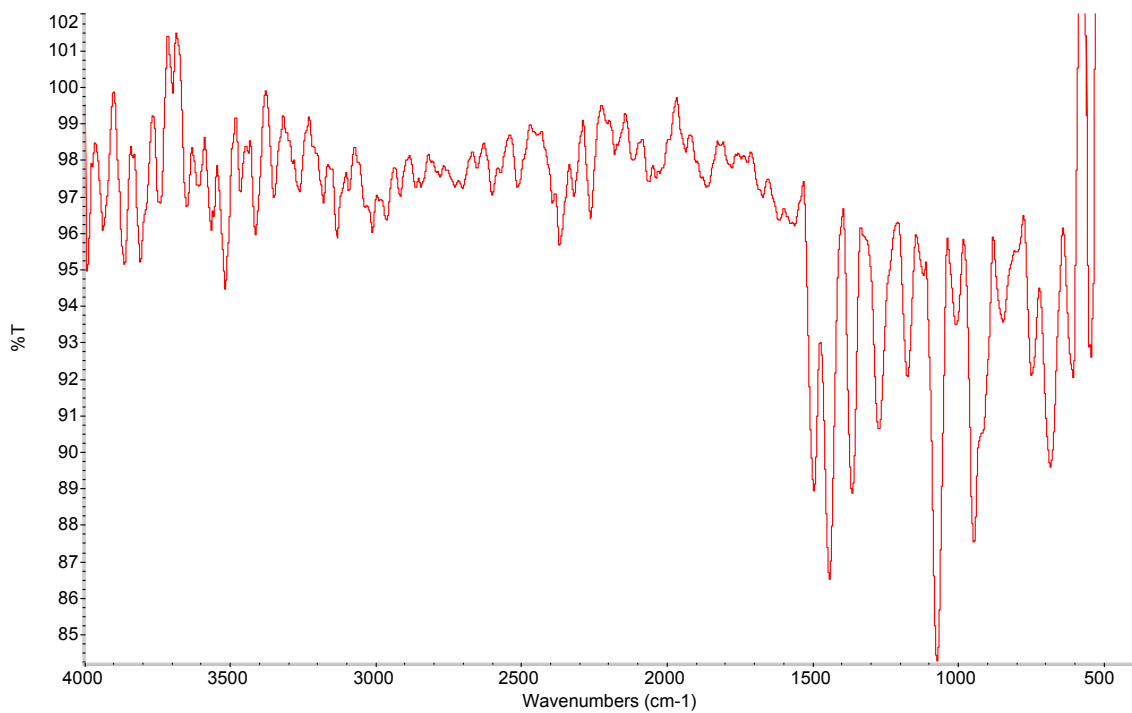


Figure S16. FT-IR (neat-ATR) spectrum of compound Ph-2EDOTV (**5**).

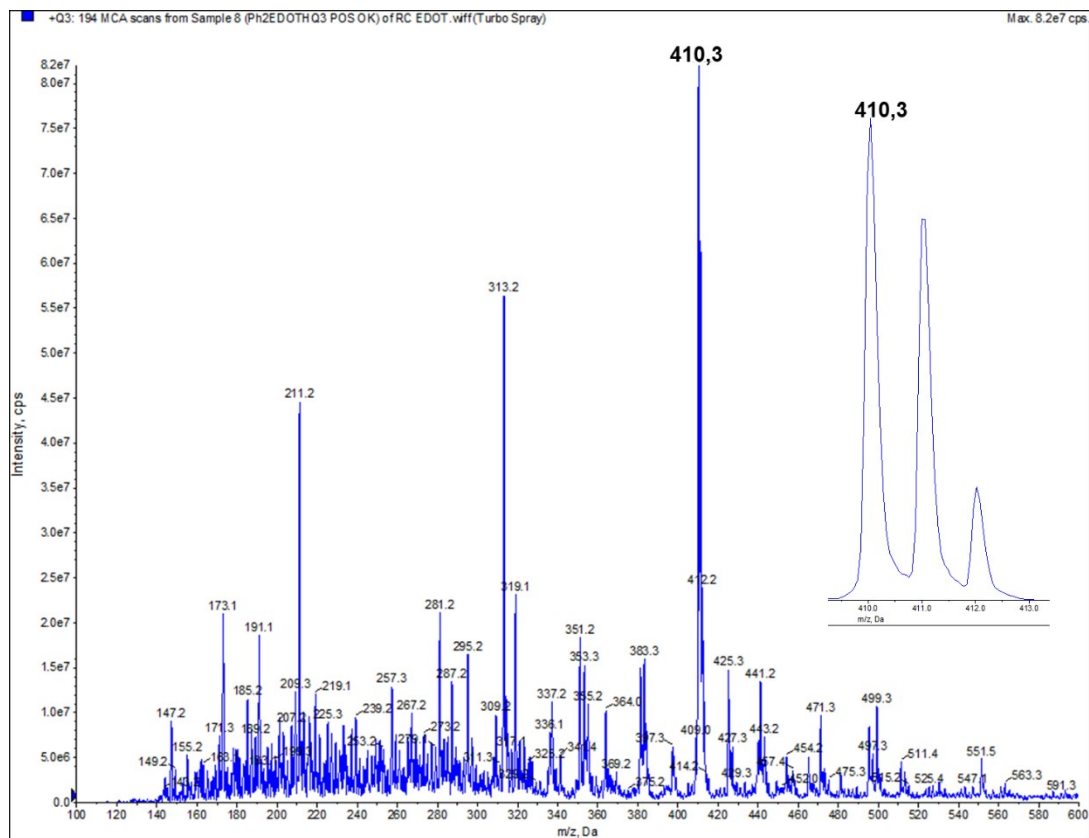


Figure S17. MS (ESI-QTOF) spectrum of compound Ph-2EDOTV (**5**).

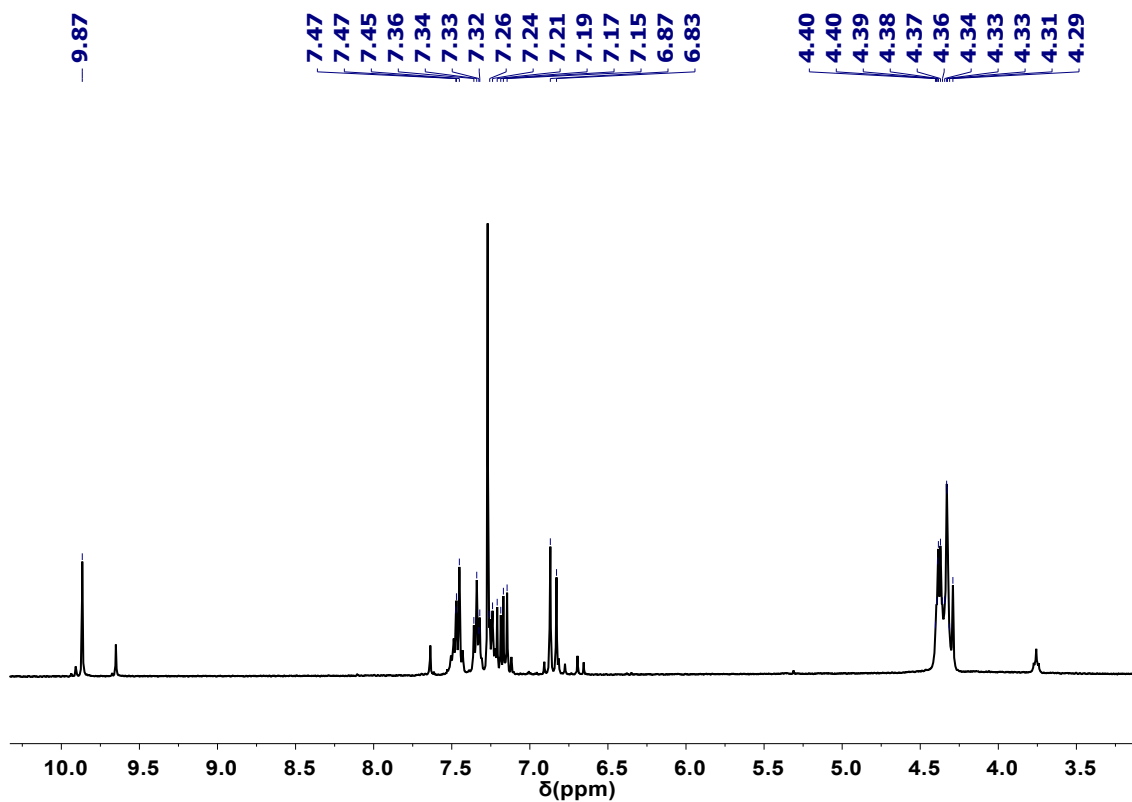


Figure S18. ¹H NMR (400 MHz, CDCl₃) spectrum of compound **S12**.

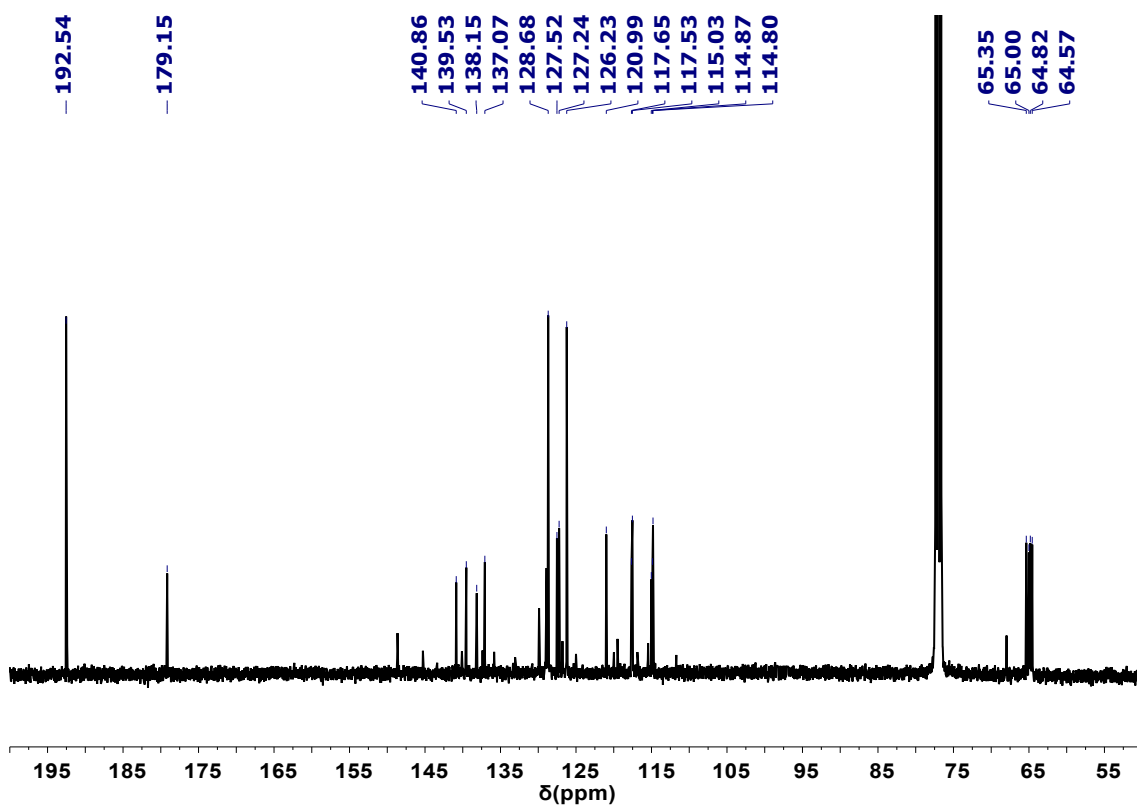


Figure S19. ^{13}C NMR (100 MHz, CDCl_3) spectrum of compound S12.

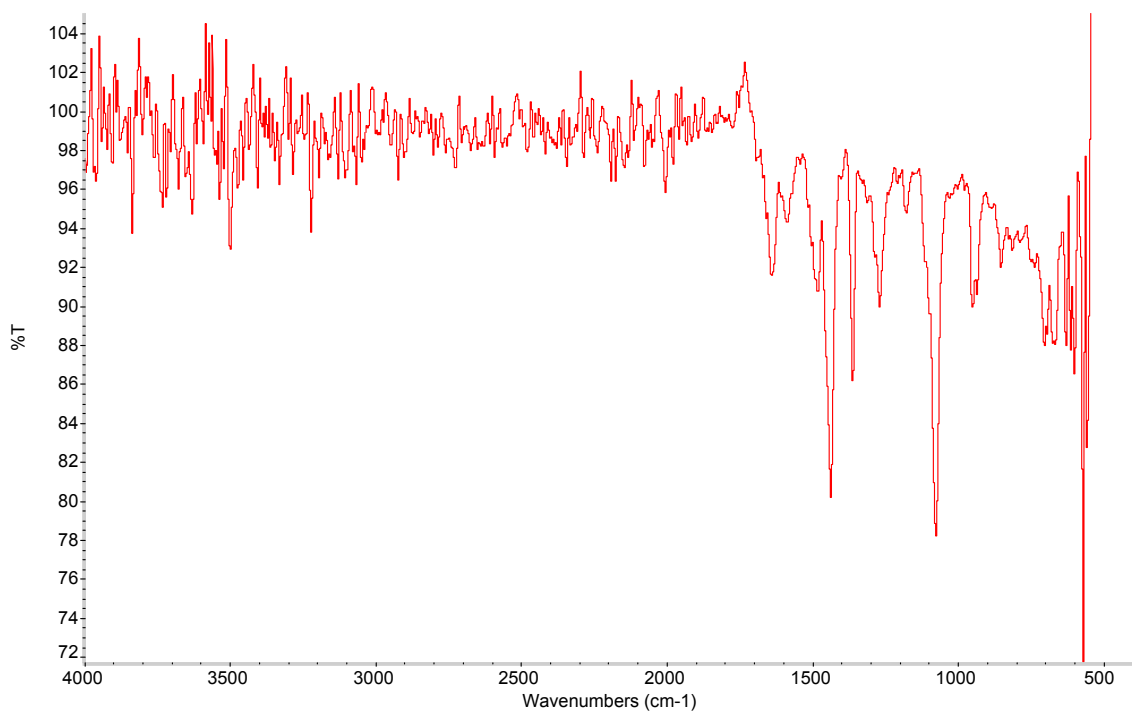


Figure S20. FT-IR (neat-ATR) spectrum of compound S12.

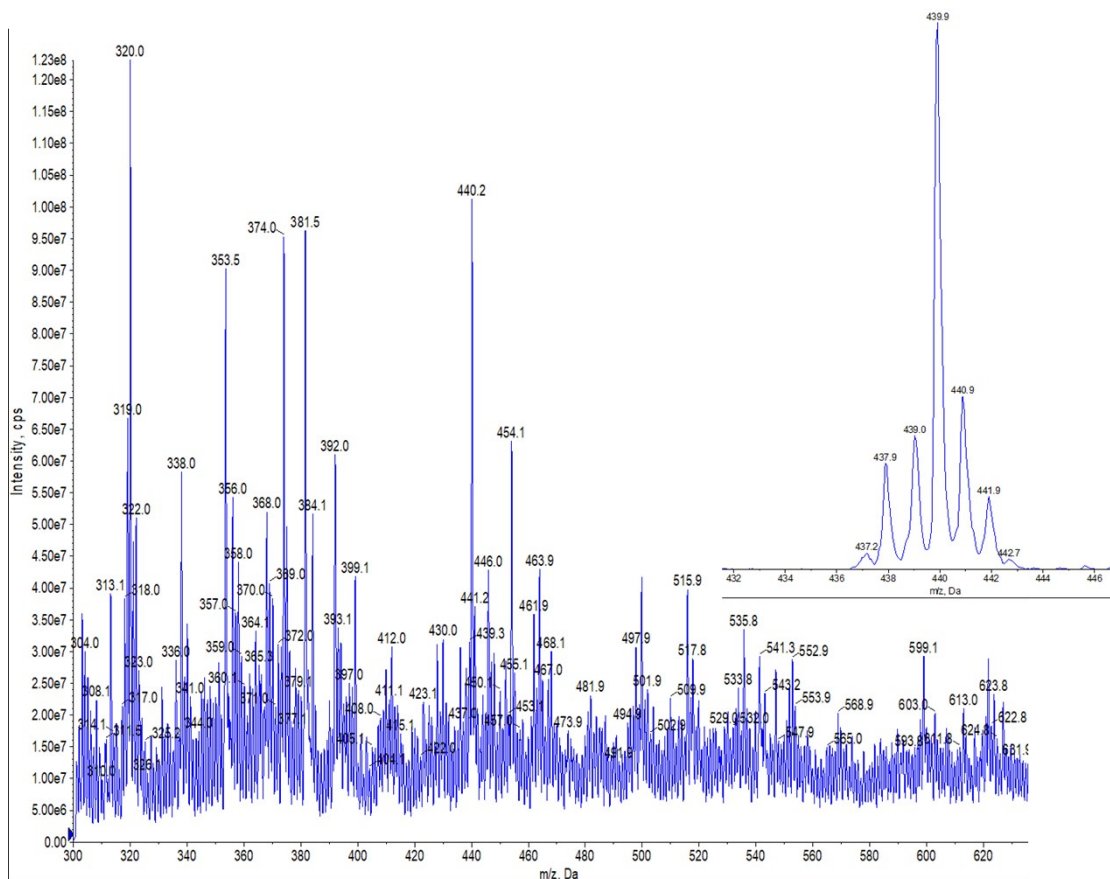


Figure S21. MS (ESI-QTOF) spectrum of compound **S12**.

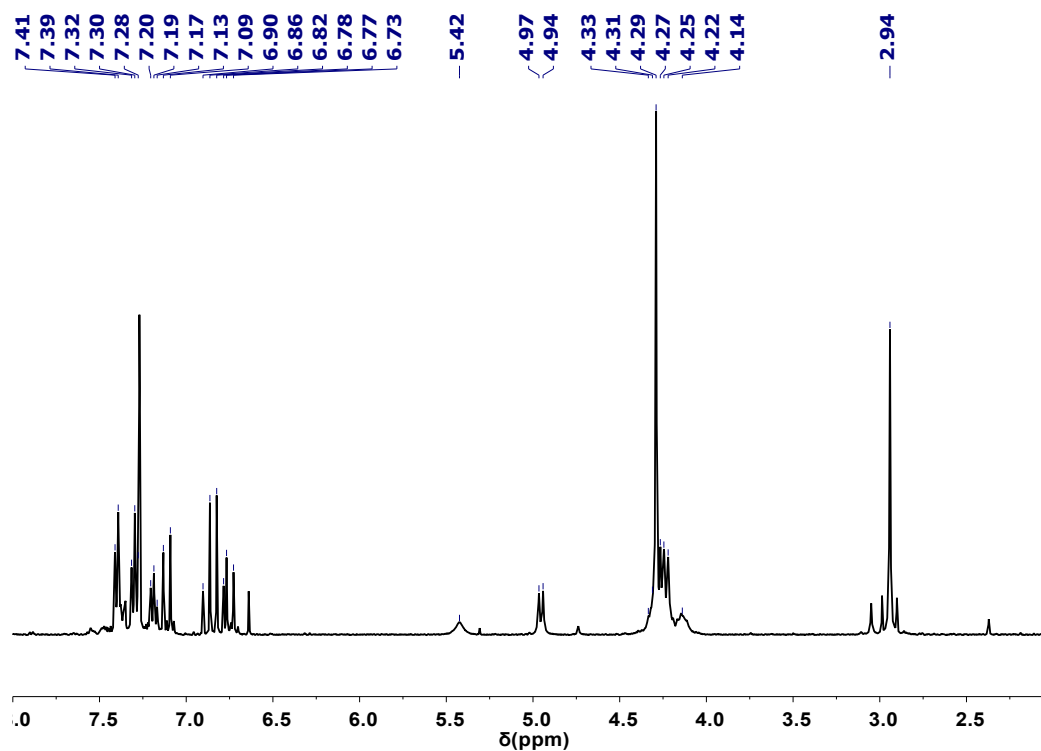


Figure S22. ^1H NMR (400 MHz, $\text{CDCl}_3/\text{CS}_2$ 1:1) spectrum of compound **Ph-2EDOTV-C₆₀ (6)**.

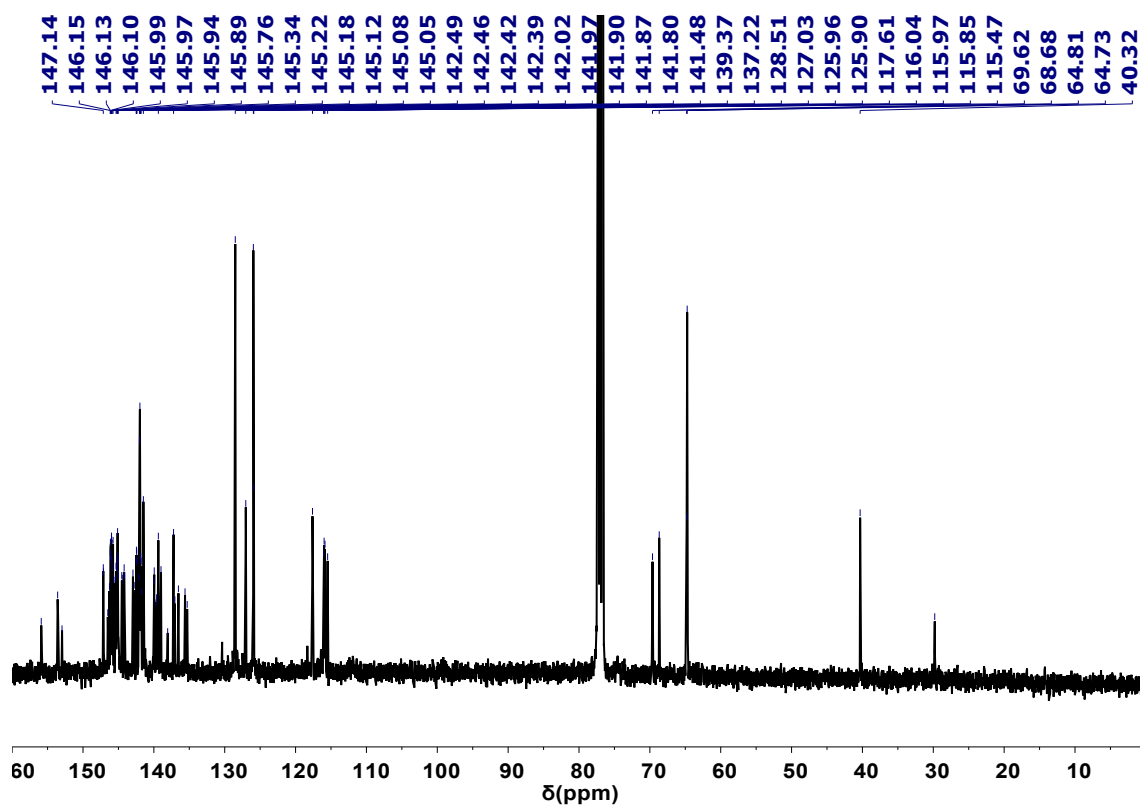


Figure S23. ^{13}C NMR (100 MHz, $\text{CDCl}_3/\text{CS}_2$ 1:1) spectrum of compound Ph-2EDOTV- C_{60} (**6**).

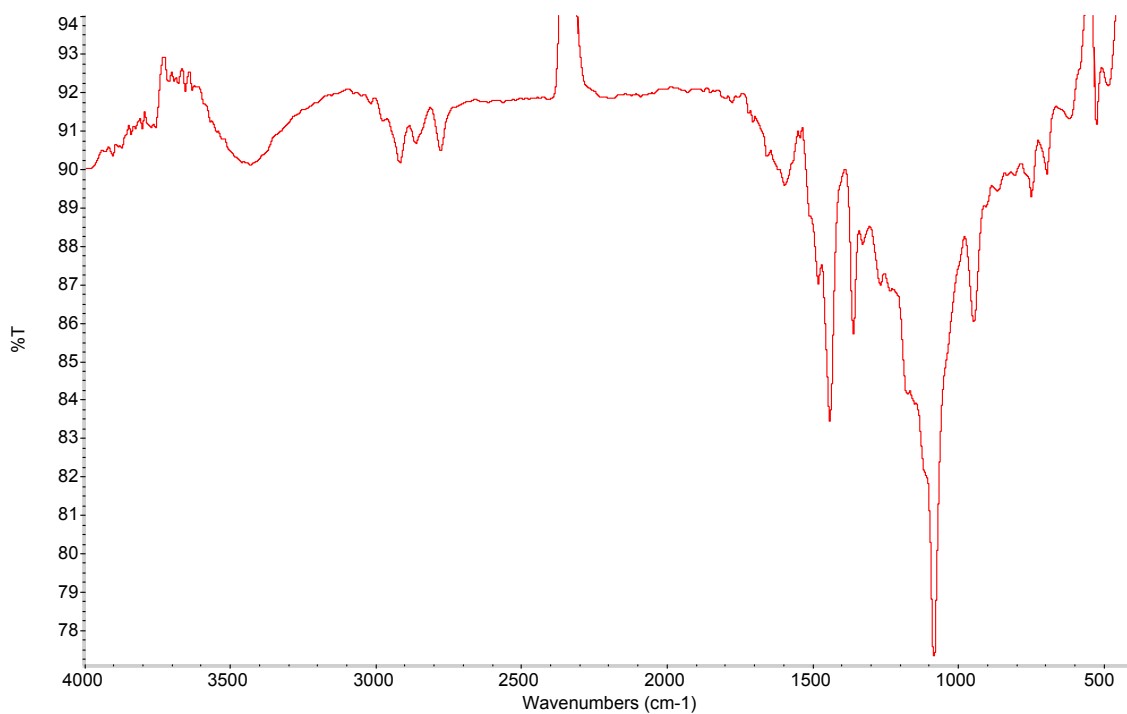


Figure S24. FT-IR (KBr) spectrum of compound Ph-2EDOTV- C_{60} (**6**).

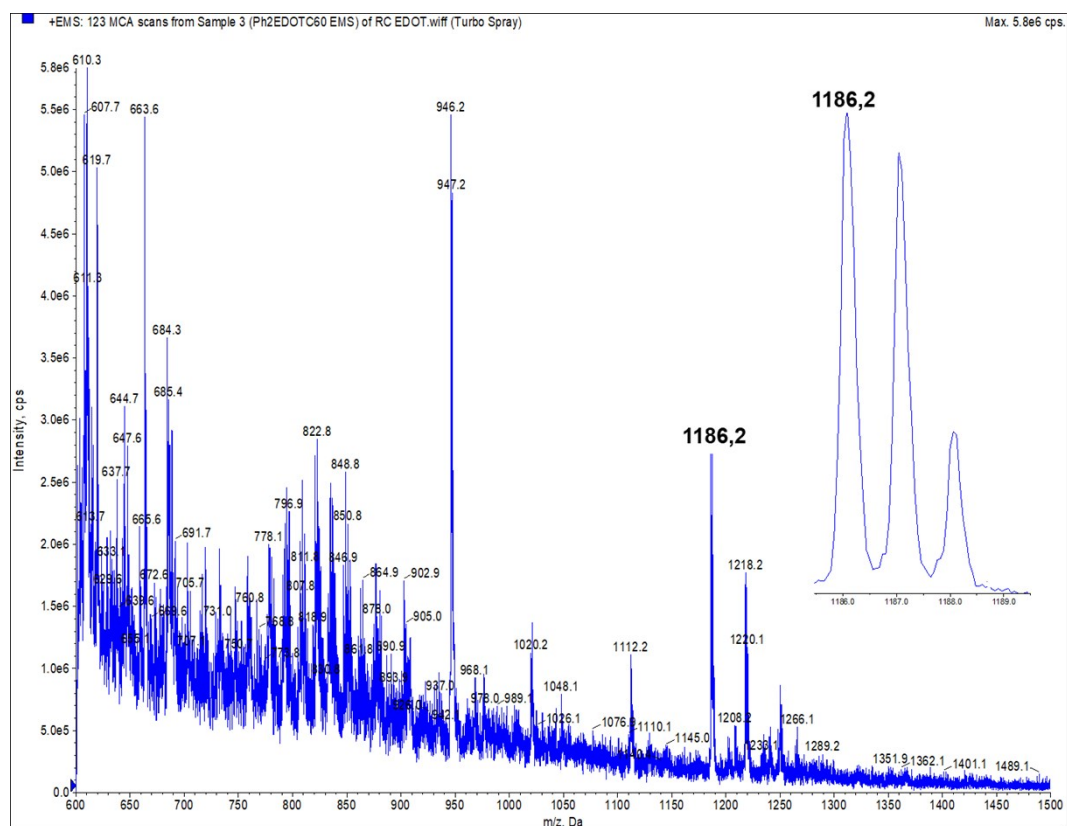


Figure S25. MS (ESI-QTOF) spectrum of compound Ph-2EDOTV-C₆₀ (6).

3. Computational Methods.

Theoretical calculations were performed within the density functional theory (DFT) framework through the Gaussian-16. A03 suite of programs.⁴ Minimum-energy molecular structures were obtained after full-geometry optimization using the popular hybrid exchange-correlation B3LYP⁵ functional with the Dunning's correlation-consistent polarized double-zeta cc-pVDZ⁶ basis set for non-metal atoms and the effective core potential LANL2DZ⁷ basis set for zinc. Solvent effects were included by means of the polarizable continuum model (PCM)^{8,9} with dichloromethane, toluene and benzonitrile as solvents. Charged species as well as the lowest-lying triplet state were optimized by using the unrestricted version of B3LYP (UB3LYP). Radical cations and anions were calculated as doublet species whereas the dication and dianion of **1** were computed both as closed-shell singlet and open-shell triplet species. For **1**²⁺, the triplet resulted to be 2.20 kcal mol⁻¹ more stable than the singlet. For **1**²⁻, the closed-shell singlet was calculated 1.68 kcal mol⁻¹ more stable than the triplet. Ionization energies (IE) and electron affinities (EA) were calculated as the difference between the total energies of the charged and neutral species at their respective minimum-energy geometry. Time-dependent DFT (TDDFT)^{10,11} calculations of the lowest-lying singlet and triplet excited states were performed to unveil the nature of the electronic excitations giving rise to the absorption spectra of triad **1** and its constituting molecular fragments. Molecular orbitals and spin densities were plotted by using the Chemcraft 1.8 software.¹²

4. Molecular geometry and orbitals

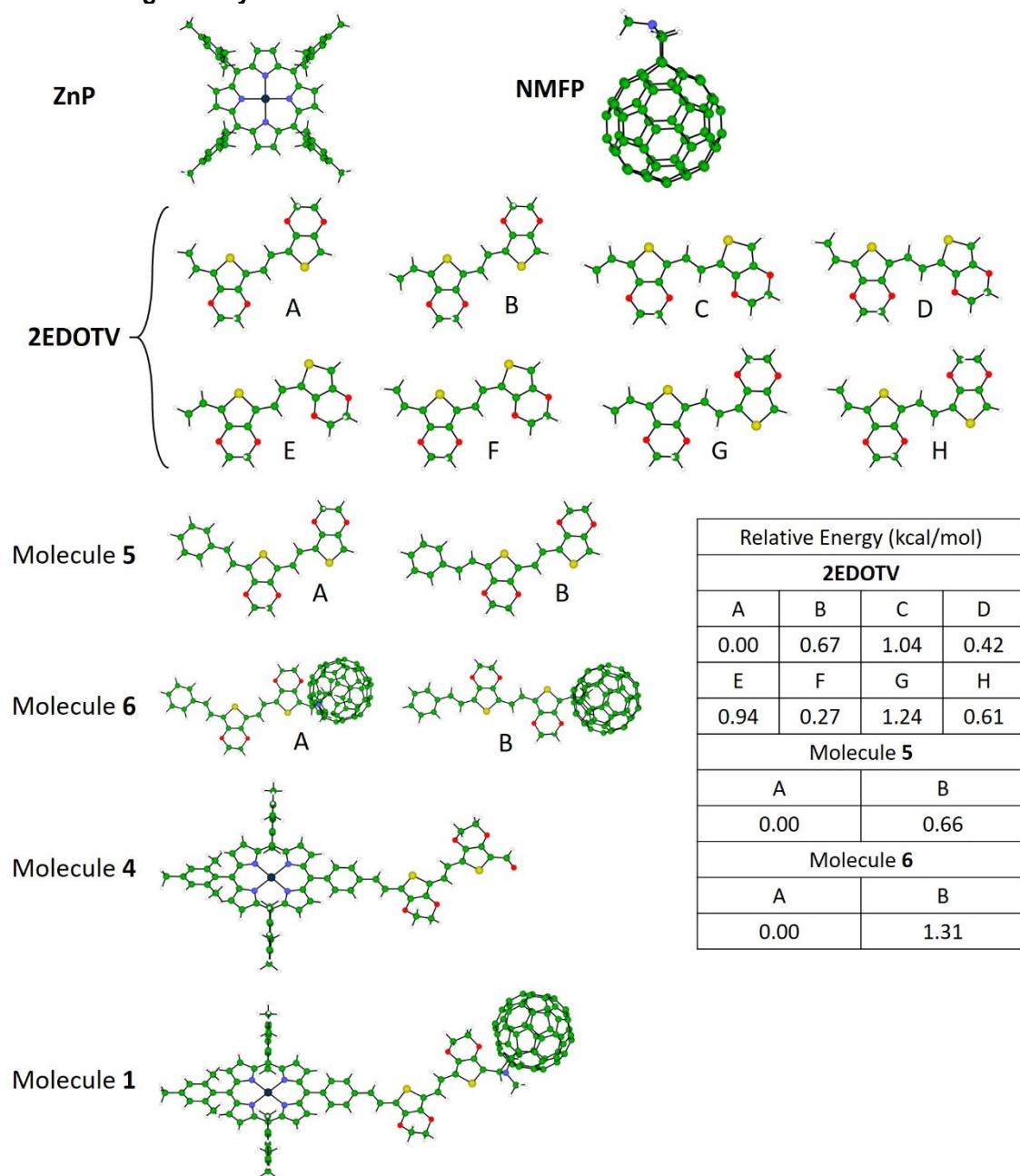


Figure S26. Minimum-energy structures calculated for relevant molecules at the B3LYP/cc-pVDZ+LANL2DZ(Zn) level of theory including solvent effects (dichloromethane in PCM). The relative energies of different conformations are summarized.

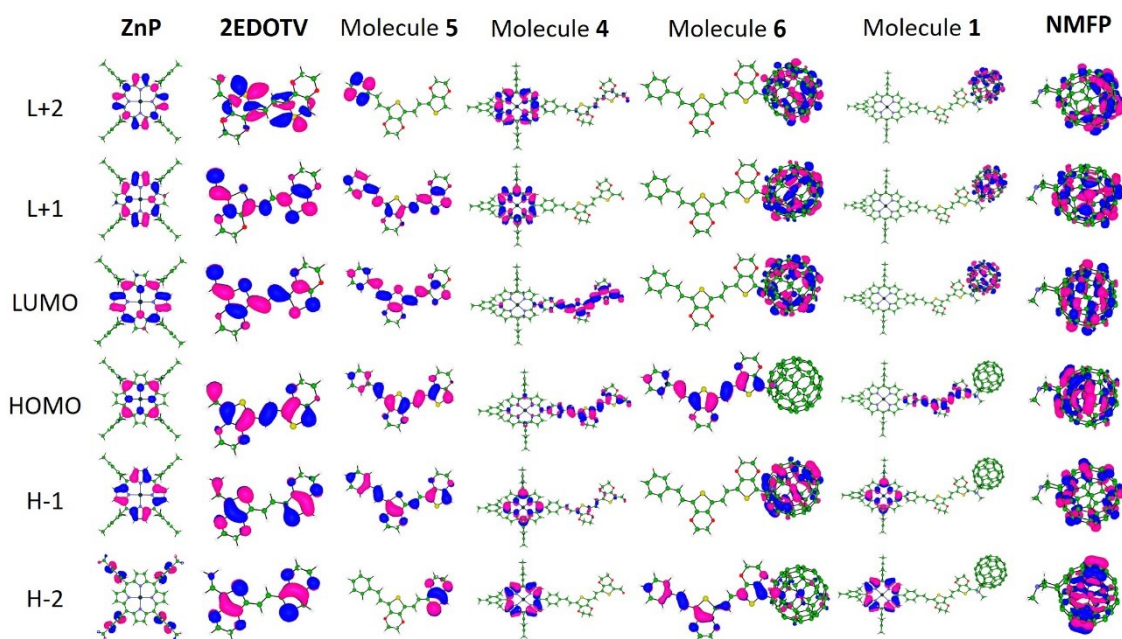


Figure S27. Frontier molecular orbital contours (isovalue = ± 0.03) calculated at the B3LYP/(cc-pVDZ+LANL2DZ(Zn))+PCM(dichloromethane) level of theory.

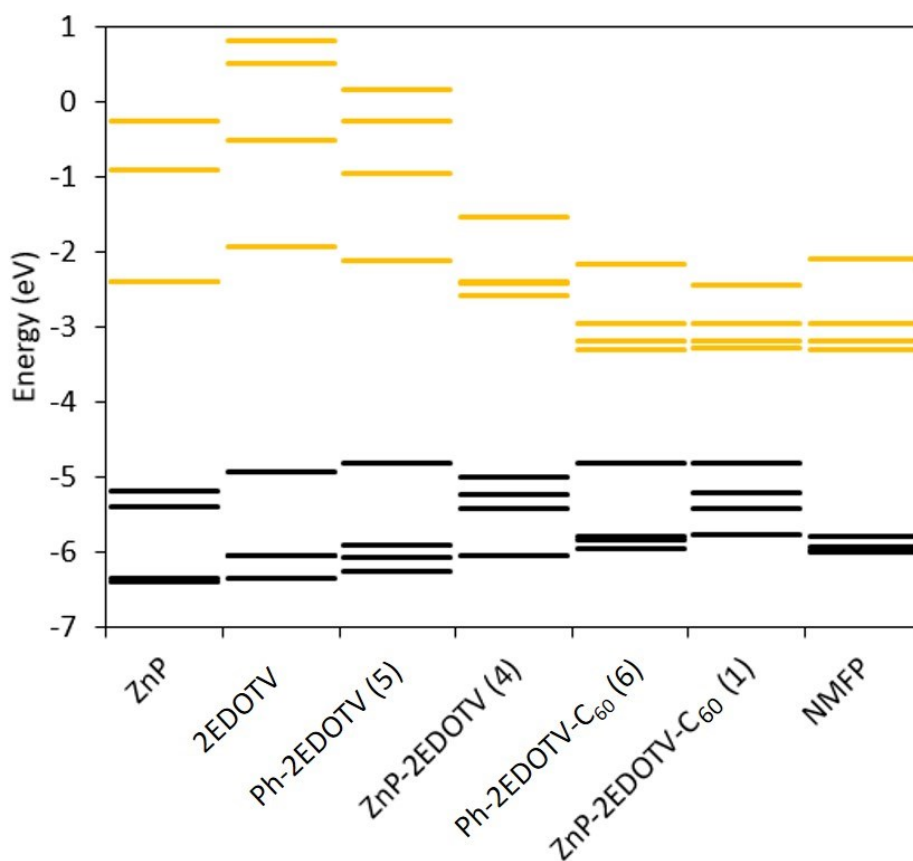


Figure S28. Energy diagram of the highest-occupied and lowest-unoccupied molecular orbitals calculated at the B3LYP/(cc-pVDZ+LANL2DZ(Zn))+PCM(dichloromethane) level of theory.

5. Electrochemical properties and calculated Mulliken charges

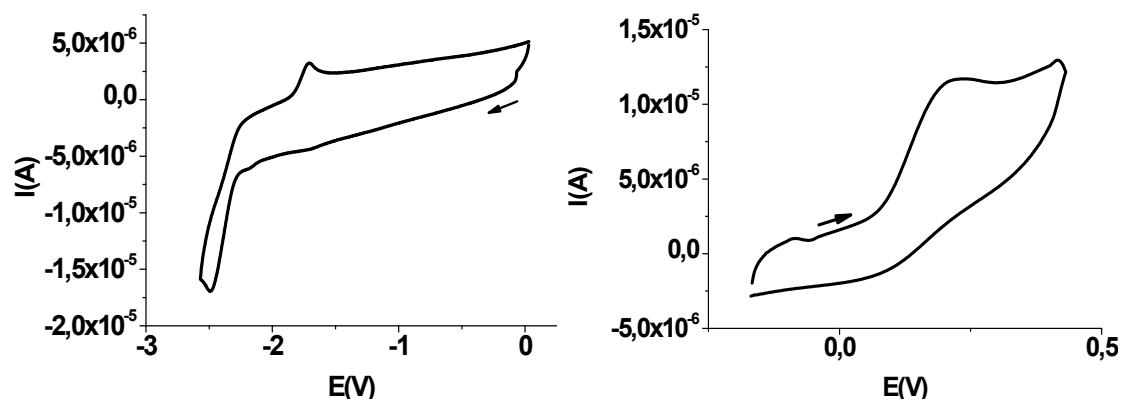


Figure S29. Cyclic voltammetry of compound Ph-2EDOTV (5).

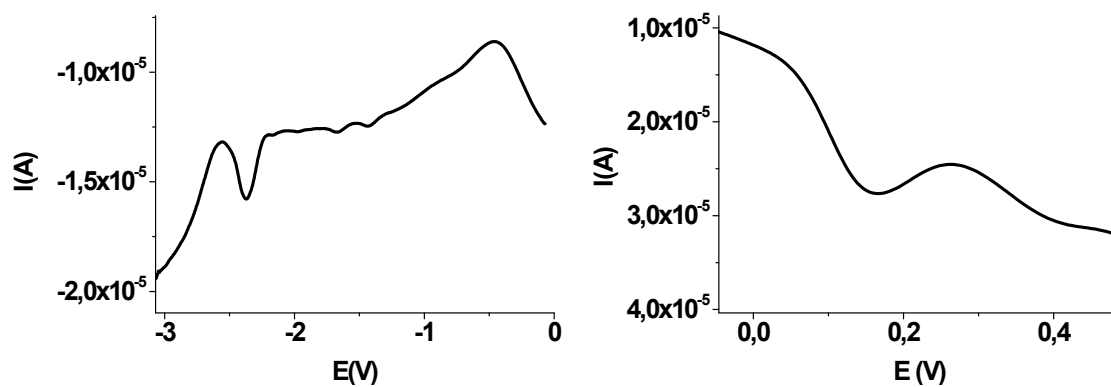


Figure S30. Oyster-Young square-wave voltammetry of compound Ph-2EDOTV (5).

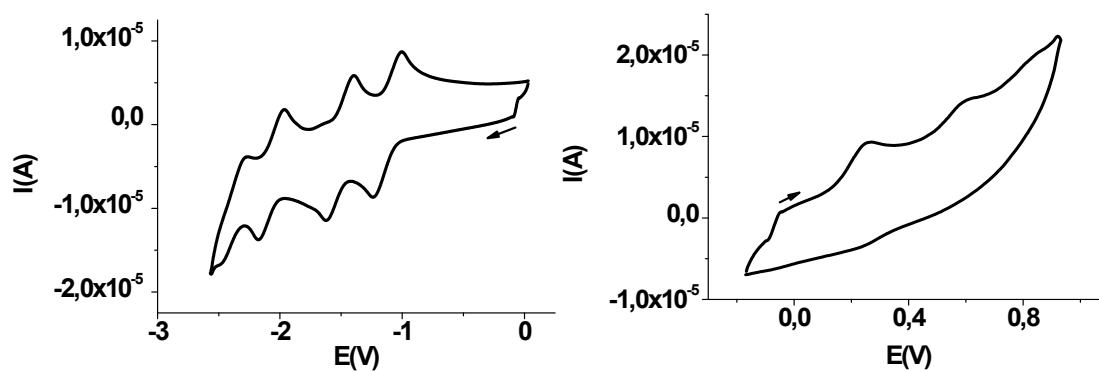


Figure S31. Cyclic voltammetry of compound Ph-2EDOTV-C₆₀ (6).

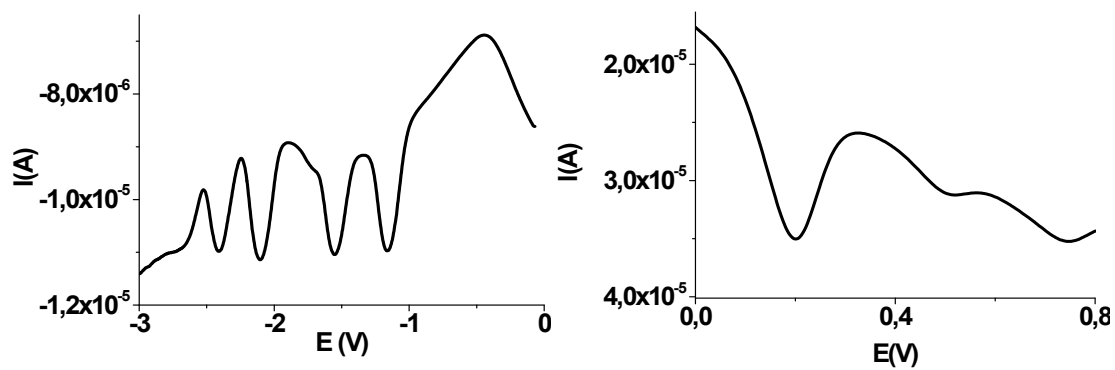


Figure S32. Oyster-Young square-wave voltammetry of compound Ph-2EDOTV-C₆₀ (6).

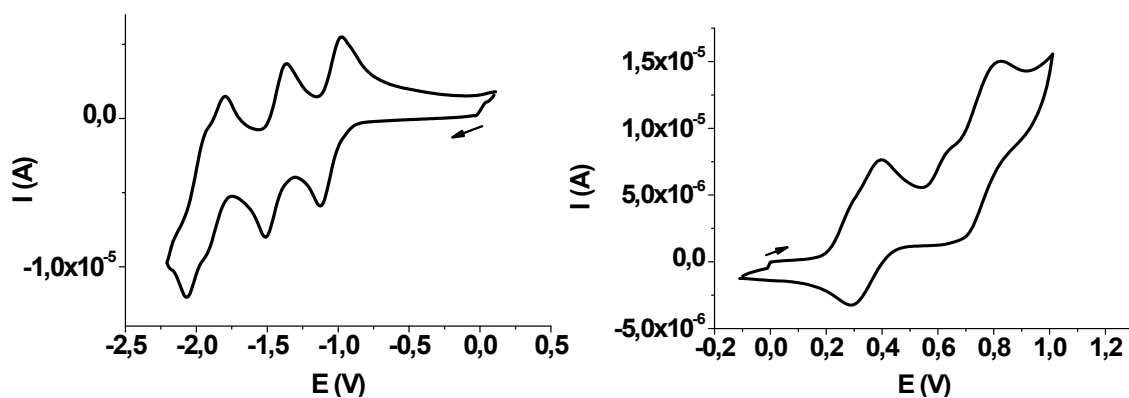


Figure S33. Cyclic voltammetry of compound ZnP-2EDOTV-C₆₀ (1).

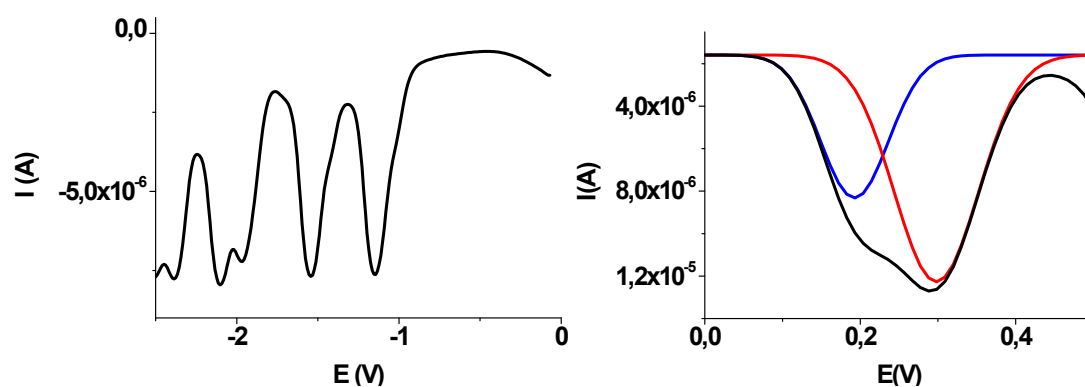


Figure S34. Oyster-Young square-wave voltammetry of compound ZnP-2EDOTV-C₆₀ (1).

Table S1. Mulliken net charges (in elementary charge e units) accumulated on the three molecular moieties (ZnP, 2EDOTV and NMFP) of triad **1** in neutral and charged states computed at the B3LYP/(cc-pVDZ+LANL2DZ(Zn))+PCM(dichloromethane) level.

	ZnP	Ph-2EDOTV	NMFP
Neutral	0.08	-0.04	-0.04
Cation	0.15	0.80	0.05
Dication	1.02	0.90	0.08
Anion	0.07	-0.06	-1.01
Dianion	0.07	-0.08	-1.99

6. Absorption and emission properties

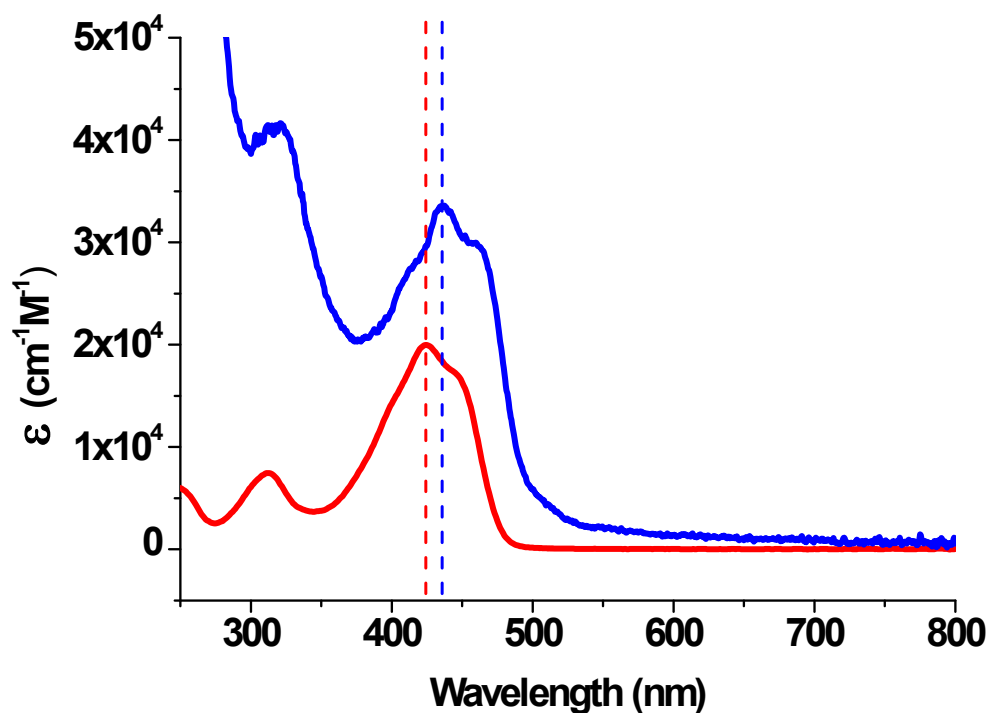


Figure S35. UV-visible absorption spectra of Ph-2EDOTV (**5**, red line) and Ph-2EDOTV-C₆₀ (**6**, blue line) in dichloromethane solution. Concentration: 10⁻⁵ M.

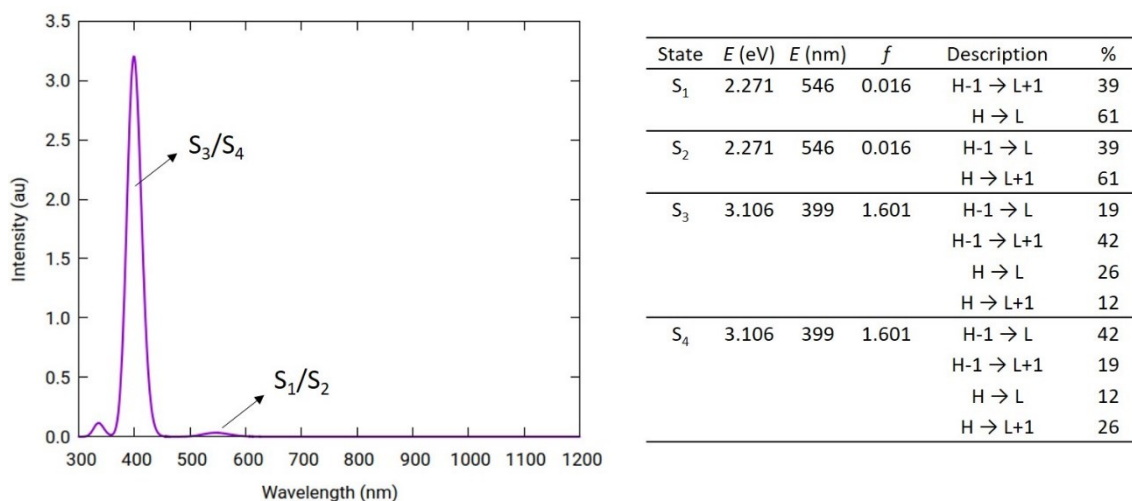


Figure S36. Simulated absorption spectrum of **ZnP** calculated at the TD-B3LYP/(cc-pVDZ+LANL2DZ(Zn))+PCM(dichloromethane) level. The energy, oscillator strength (*f*) and nature in terms of mono-electronic excitations of the singlet → singlet (S₀ → S_n) electronic transitions are summarized.

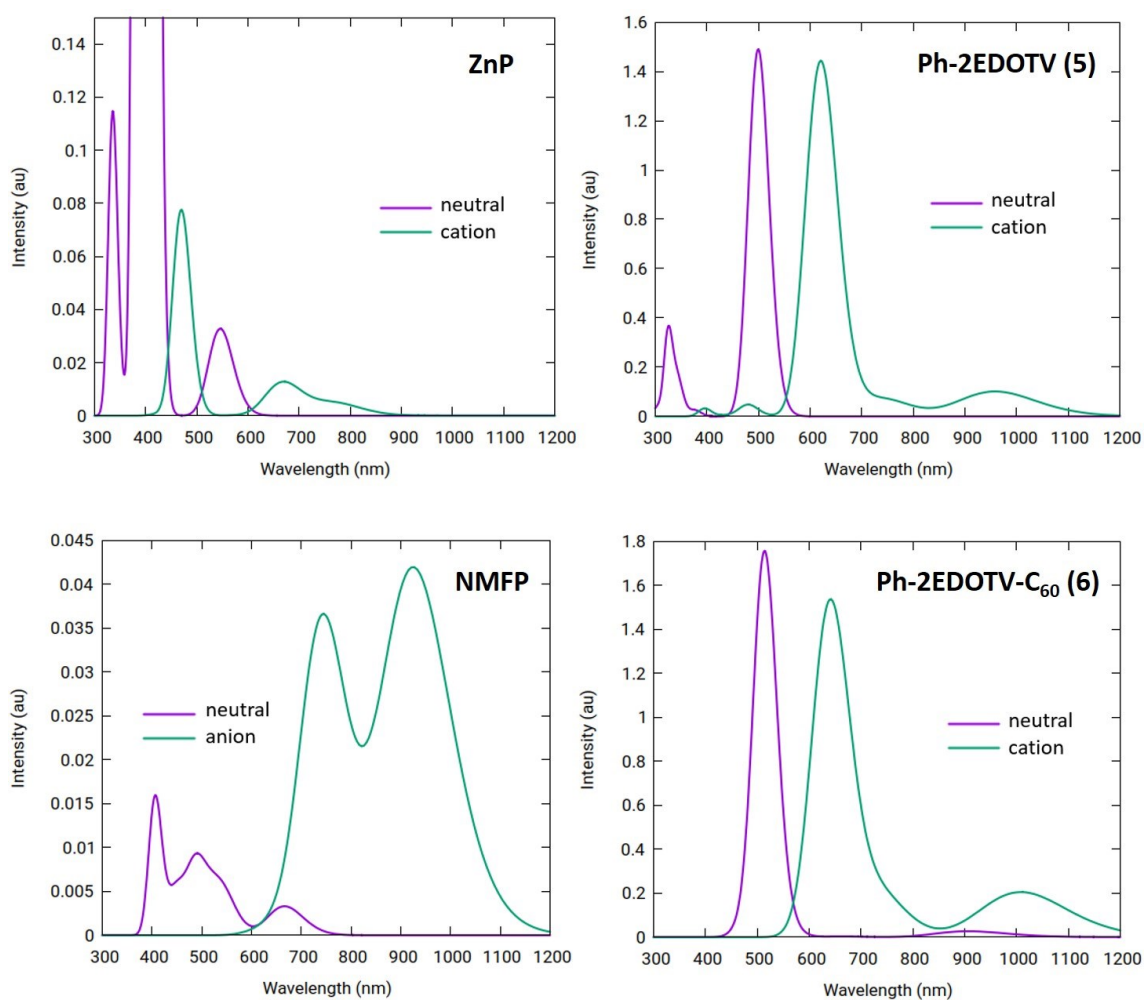


Figure S37. Simulated absorption spectra of **ZnP**, Ph-2EDOTV (**5**), **NMFP** and Ph-2EDOTV-C₆₀ (**6**) calculated at the TD-B3LYP/(cc-pVDZ+LANL2DZ(Zn))+PCM(dichloromethane) level in their neutral and cation or anion states.

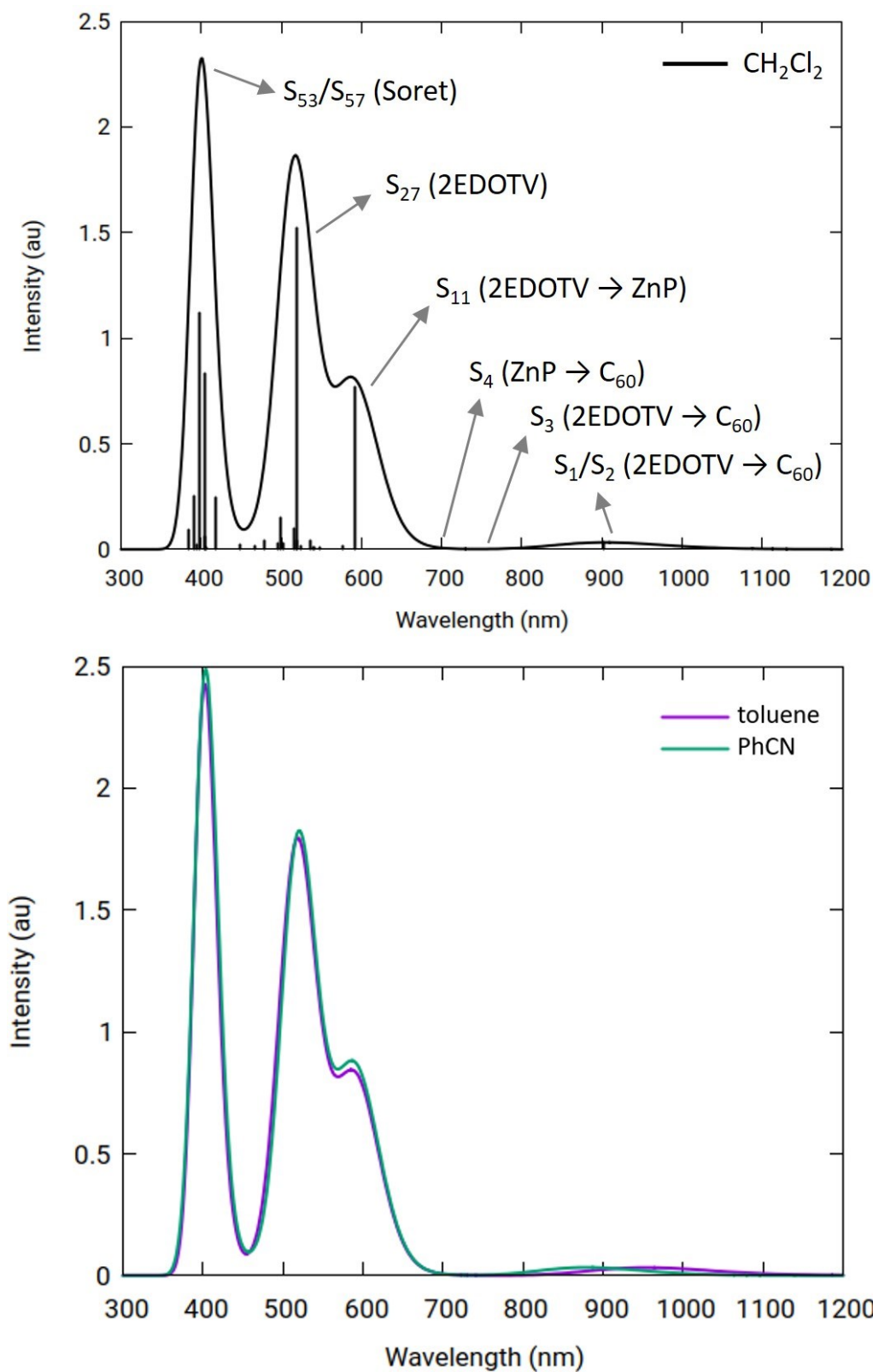


Figure S38. Simulated absorption spectrum of triad 1 calculated at the TD-B3LYP/(cc-pVDZ+LANL2DZ(Zn))+PCM level in three solvent conditions (dichloromethane, toluene and benzonitrile). The nature of the electronic states that lead to the most characteristic bands is indicated in CH₂Cl₂ conditions (see Table S2 for further details of the transitions).

Table S2. Vertical excitation energy (E), oscillator strength (f) and nature in terms of mono-electronic excitations calculated for the $S_0 \rightarrow S_n$ transitions of triad **1** at the TD-B3LYP/(cc-pVDZ+LANL2DZ(Zn))+PCM(dichloromethane) level of theory.

State	E (eV)	E (nm)	f	Description ^a	%
S_1	1.263	981	0.0020	H \rightarrow L	99
S_2	1.375	902	0.0317	H \rightarrow L+1	99
S_3	1.622	765	0.0001	H \rightarrow L+2	99
S_4	1.786	694	0.0001	H-1 \rightarrow L	99
S_{11}	2.097	591	0.7667	H \rightarrow L+3	90
S_{27}	2.391	523	1.5196	H \rightarrow L+5	83
S_{53}	3.066	404	0.8304	H-4 \rightarrow L+3	20
				H-2 \rightarrow L+4	35
				H-1 \rightarrow L+3	20
S_{57}	3.111	399	1.1214	H-2 \rightarrow L+3	29
				H-2 \rightarrow L+5	32
				H-1 \rightarrow L+4	27

^a H and L denote HOMO and LUMO, respectively.

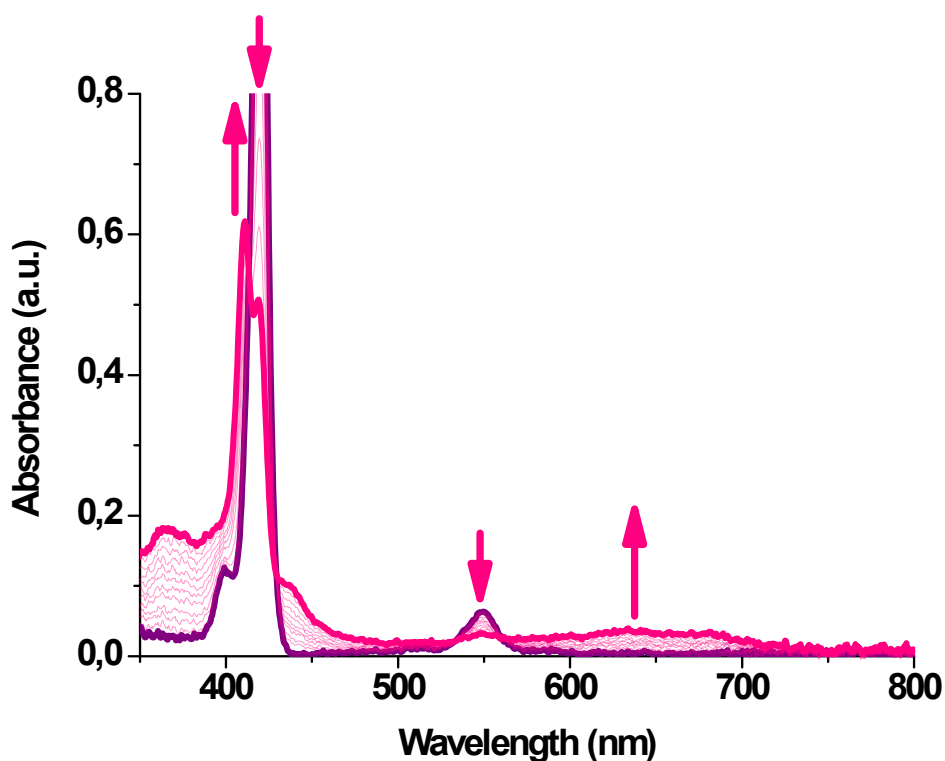


Figure S39. UV-Vis absorption spectra of neutral (purple) and oxidized species (pink) of **ZnP**, in dichloromethane solution, obtained upon oxidation with FeCl_3 .

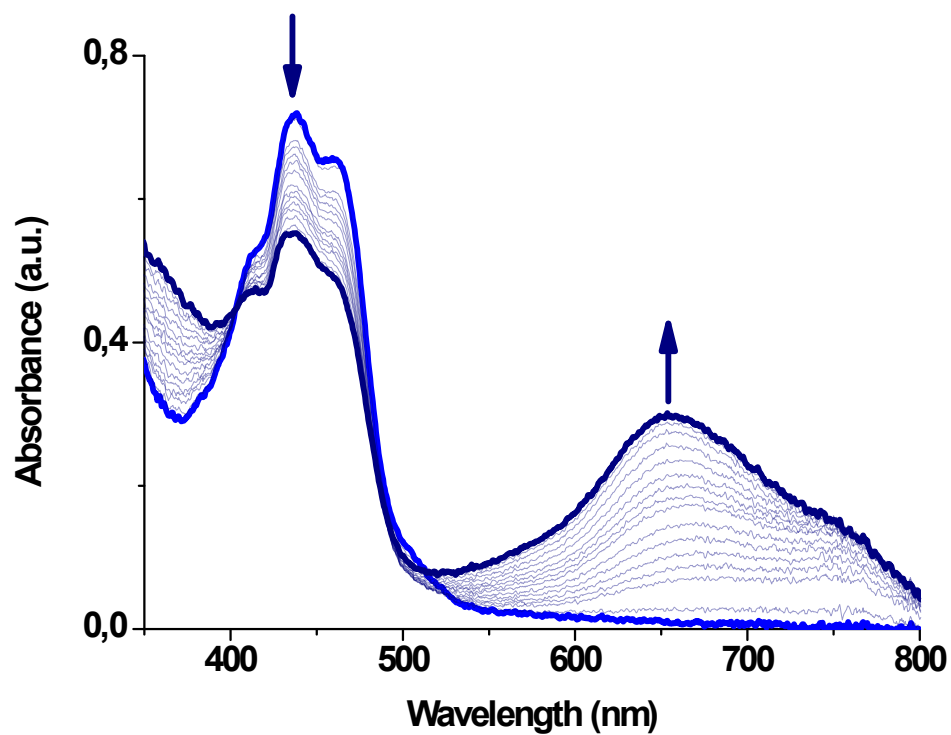


Figure 40. UV-Vis absorption spectra of neutral (light blue) and oxidized species (dark blue) of Ph-2EDOTV-C₆₀ (**6**), in dichloromethane solution, obtained upon oxidation with FeCl₃.

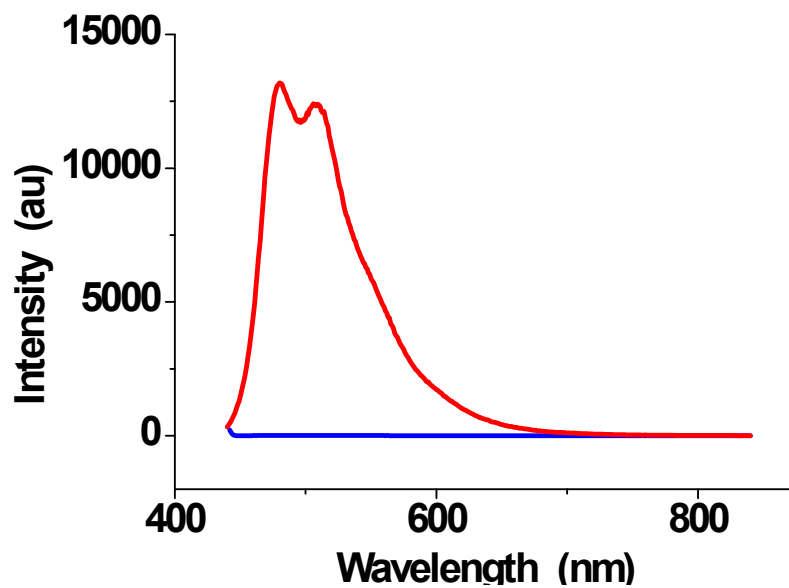


Figure S41. Steady-state fluorescence spectra of Ph-2EDOTV (**5**, red line) and Ph-2EDOTV-C₆₀ (**6**, blue line) in toluene. Concentration 10⁻⁵ M.

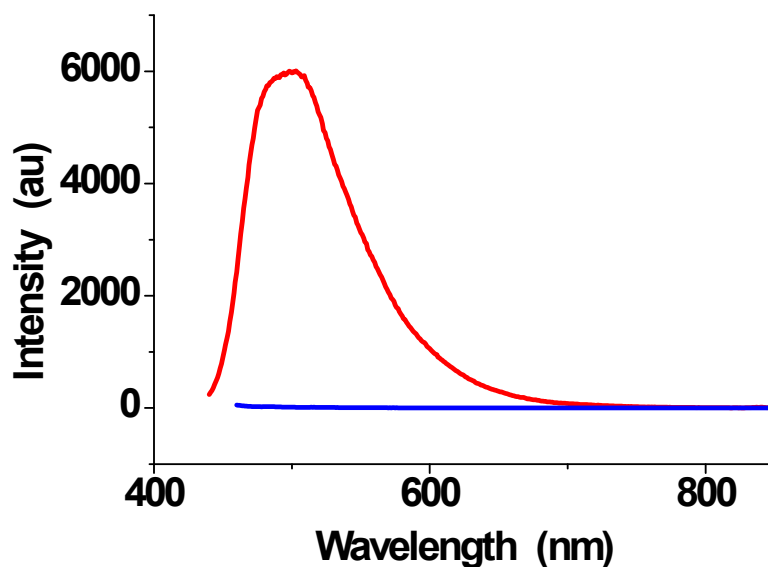


Figure S42. Steady-state fluorescence spectra of Ph-2EDOTV (**5**, red line) and Ph-2EDOTV-C₆₀ (**6**, blue line) in benzonitrile. Concentration 10⁻⁵ M.

7. Transient absorption spectra

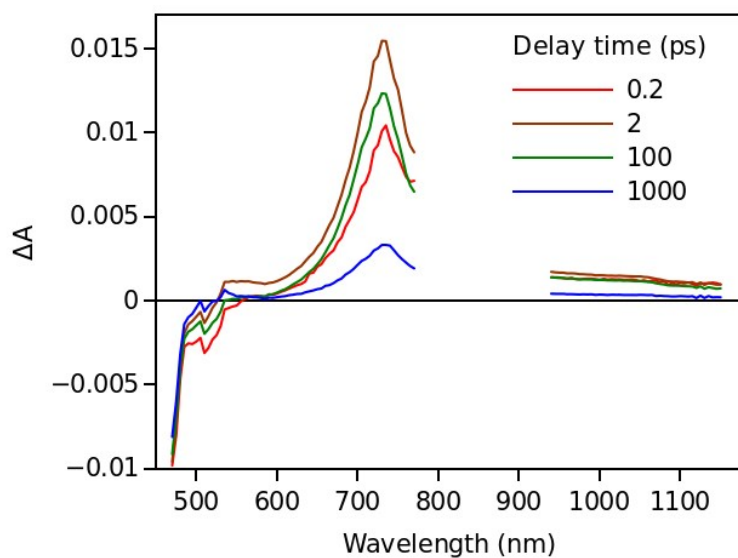


Figure S43. Time-resolved transient absorption spectra of Ph-2EDOTV (**5**) in PhCN. Excitation wavelength was 420 nm. The singlet-excited state of **5** has a strong absorption band around 730 nm, which is formed almost instantly and decays with time constant of 640 ps.

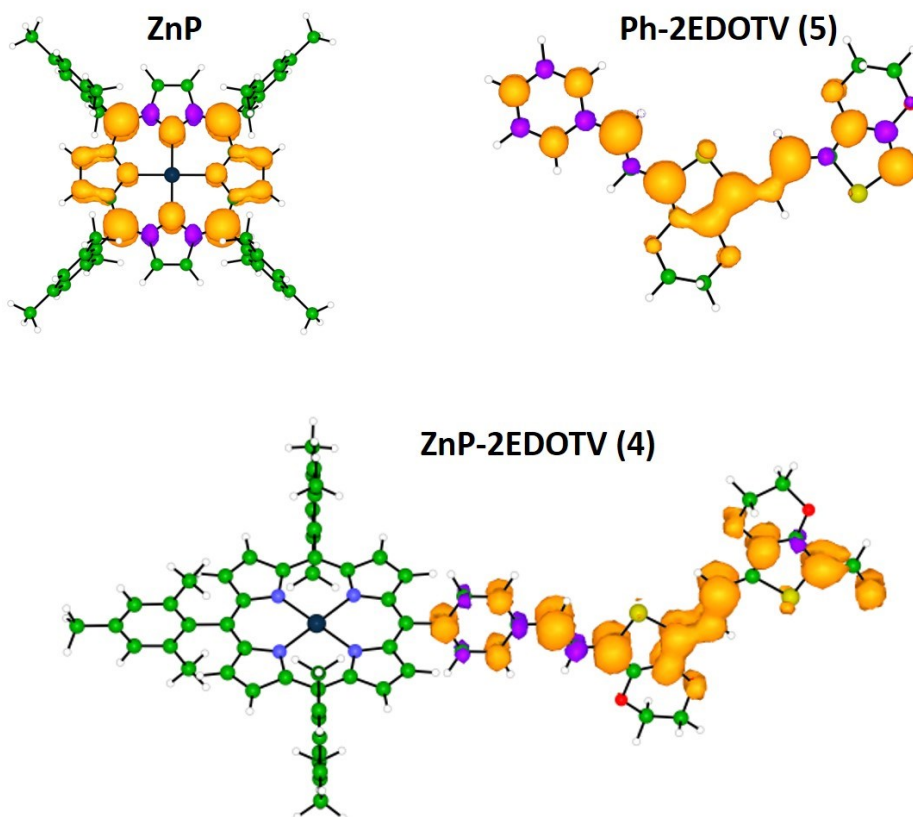


Figure S44. Spin density (isovalue = 0.003) calculated for the lowest-lying triplet state of **4** and constituting **ZnP** and **5** systems at the UB3LYP/(cc-pVDZ+LANL2DZ(Zn))+PCM(toluene) level.

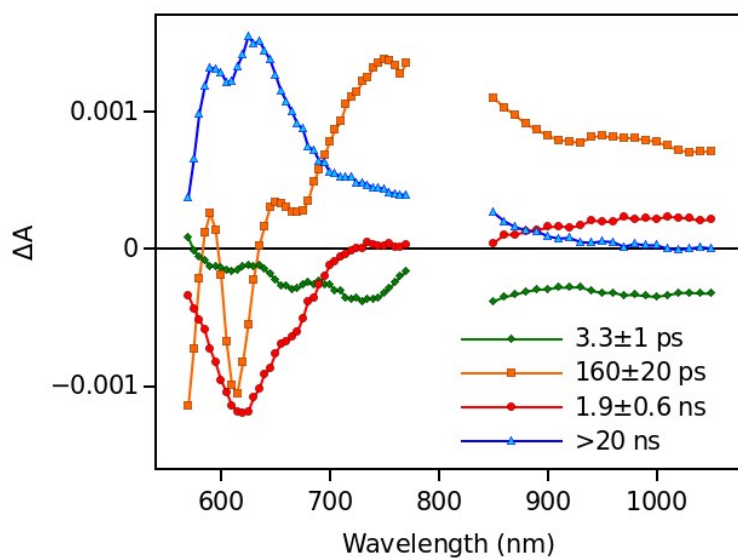


Figure S45. Decay-associated TA component spectra of ZnP-2EDOTV (**4**) in PhCN excited at 560 nm. The time constants associated with the components are indicated in the plot.

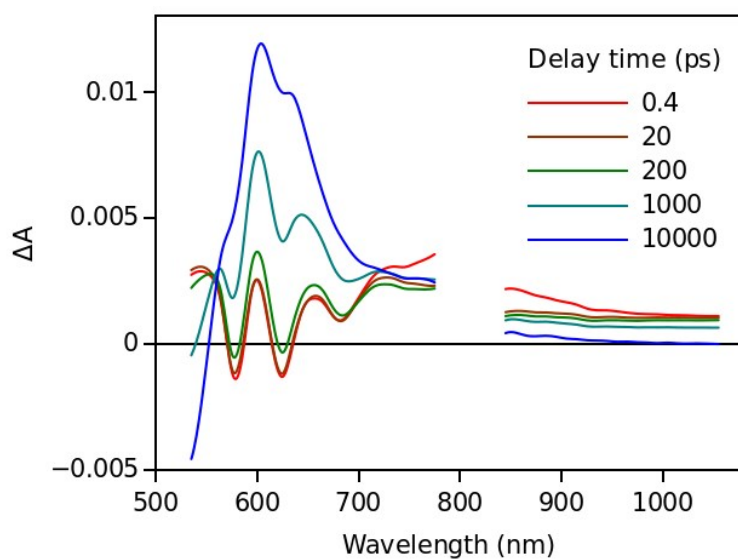


Figure S46. Time-resolved transient absorption spectra of ZnP-2EDOTV (**4**) in toluene. Excitation wavelength was 495 nm.

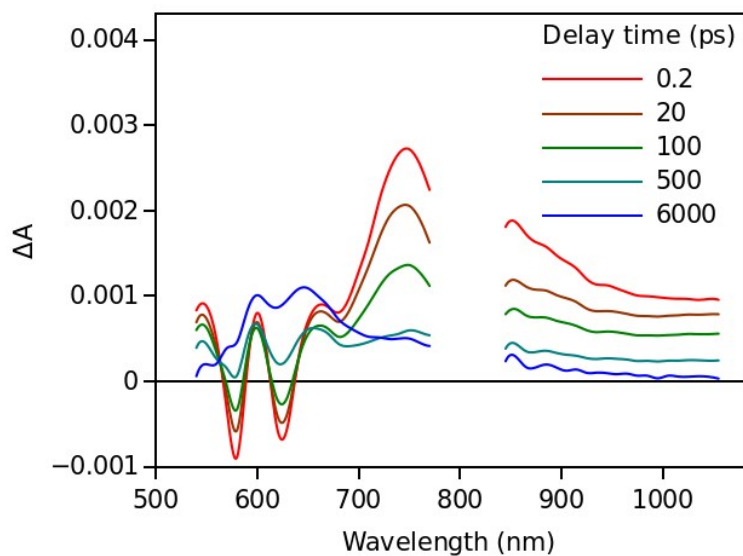


Figure S47. Time-resolved transient absorption spectra of ZnP-2EDOTV (**4**) in PhCN excited at 495 nm.

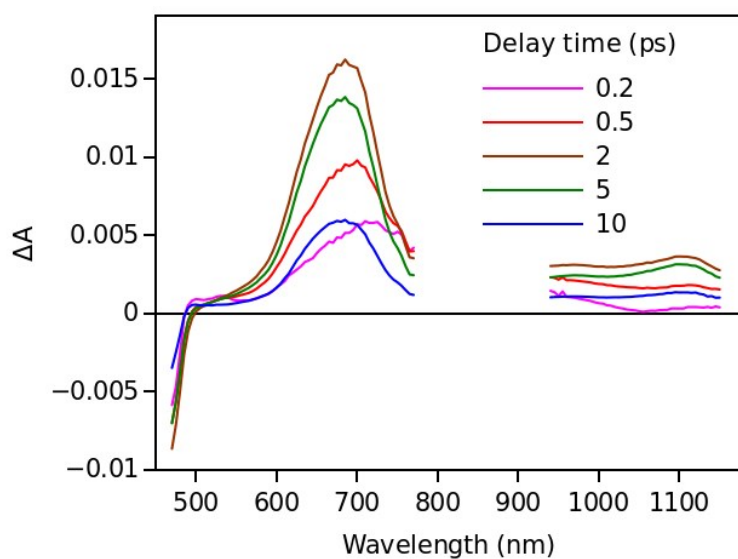


Figure S48. Time-resolved transient absorption spectra of Ph-2EDOTV-C₆₀ (**6**) in PhCN excited at 420 nm.

8. References

1. K. N. Shivananda, I. Cohen, E. Borzin, Y. Gerchikov, M. Firstenberg, O. Solomeshch, N. Tessler and Y. Eichen, *Adv. Func. Mater.* 2012, **22**, 1489-1501.
2. S. Wagner, M. Accorsi and J. Rademann, *Chem. Eur. J.*, 2017, **23**, 15387–15395.
3. M. Turbiez, P. Frere and J. Roncali, *Tetrahedron*, 2005, **61**, 3045–3053.
4. Gaussian 16, Revision A.03, M. J. Frisch, G. W. Trucks, H. B. Schlegel, G. E. Scuseria, M. A. Robb, J. R. Cheeseman, G. Scalmani, V. Barone, G. A. Petersson, H. Nakatsuji, X. Li, M. Caricato, A. V. Marenich, J. Bloino, B. G. Janesko, R. Gomperts, B. Mennucci, H. P. Hratchian, J. V. Ortiz, A. F. Izmaylov, J. L. Sonnenberg, D. Williams-Young, F. Ding, F. Lipparini, F. Egidi, J. Goings, B. Peng, A. Petrone, T. Henderson, D. Ranasinghe, V. G. Zakrzewski, J. Gao, N. Rega, G. Zheng, W. Liang, M. Hada, M. Ehara, K. Toyota, R. Fukuda, J. Hasegawa, M. Ishida, T. Nakajima, Y. Honda, O. Kitao, H. Nakai, T. Vreven, K. Throssell, J. A. Montgomery, Jr., J. E. Peralta, F. Ogliaro, M. J. Bearpark, J. J. Heyd, E. N. Brothers, K. N. Kudin, V. N. Staroverov, T. A. Keith, R. Kobayashi, J. Normand, K. Raghavachari, A. P. Rendell, J. C. Burant, S. S. Iyengar, J. Tomasi, M. Cossi, J. M. Millam, M. Klene, C. Adamo, R. Cammi, J. W. Ochterski, R. L. Martin, K. Morokuma, O. Farkas, J. B. Foresman and D. J. Fox, Gaussian, Inc., Wallingford CT, 2016.
5. A. D. Becke, *J. Chem. Phys.*, **98** (1993) 5648–5652.
6. T. H. Dunning Jr., *J. Chem. Phys.*, **90** (1989) 1007–1023.
7. J. Hay and W. R. Wadt, *J. Chem. Phys.*, **82** (1985) 270–283.
8. J. L. Pascual-Ahuir, E. Silla and I. Tuñón, *J. Comp. Chem.*, **15** (1994) 1127–1138.
9. J. Tomasi, B. Mennucci and R. Cammi, *Chem. Rev.*, **105** (2005) 2999–3093.
10. R. Bauernschmitt and R. Ahlrichs, *Chem. Phys. Lett.*, **256** (1996) 454–464.
11. M. E. Casida, C. Jamorski, K. C. Casida and D. R. Salahub, *J. Chem. Phys.*, **108** (1998) 4439–4449.
12. Chemcraft - graphical software for visualization of quantum chemistry computations.
<https://www.chemcraftprog.com>